

# Bureau of Safety and Environmental Enforcement Oil Spill Preparedness Division MARINE SCOUT Advancement

Volume 1  
Final Report

July 2023



(Photo: QinetiQ, 2022)

Ted George, Devon Barbour, George Stone

US Department of the Interior  
Bureau of Safety and Environmental Enforcement  
Oil Spill Preparedness Division



# MARINE SCOUT Advancement

Volume 1  
Final Report

OSRR # 1131  
2023 Copyright, QinetiQ, Inc.

July 2023

Authors:  
Ted George  
QinetiQ, Inc

QINETIQ

Devon Barbour  
QinetiQ, Inc

QINETIQ

George Stone  
QinetiQ, Inc

QINETIQ

Prepared under Contract# 140E121C0006  
By  
QinetiQ, Inc  
10440 Furnace Rd, Lorton, VA 22079

QINETIQ

**US Department of the Interior  
Bureau of Safety and Environmental Enforcement  
Oil Spill Preparedness Division**



## **DISCLAIMER**

### **Contracts:**

Study concept, oversight, and funding were provided by the U.S. Department of the Interior (DOI), Bureau of Safety and Environmental Enforcement (BSEE), Oil Spill Preparedness Division (OSPD), Sterling, VA, under Contract Number 140E0121C0006. This report has been reviewed by BSEE, and it has been approved for publication. The views and conclusions contained in this document are those of the authors and should not be interpreted as representing the opinions or policies of the U.S. Government, nor does mention of trade names or commercial products constitute endorsement or recommendation for use.

## REPORT AVAILABILITY

The .pdf file for this report is available through the following sources. Click on the URL and enter the appropriate search term to locate the .pdf.

Document Source	Search Term	URL
Bureau of Safety and Environmental Enforcement (BSEE) Sources: a) BSEE (2019)	Project Number – 1131	<a href="http://www.bsee.gov/research-record">www.bsee.gov/research-record</a>

## CITATION

George, Ted; Barbour, Devon; Stone, George; (QinetiQ Inc., Lorton, VA). 2023. MARINE SCOUT Advancement. Lorton, VA: U.S. Department of the Interior, Bureau of Safety and Environment Enforcement. Project No. OSRR # 1131, Contract No.: 140E121C0006.

## ABOUT THE COVER

Cover image by QinetiQ Inc., MARINE SCOUT Data Sheet 22v12, 2022.

## ACKNOWLEDGEMENTS

Copyright 2023, QinetiQ, Inc.

# GRAPHICAL ABSTRACT



## EXECUTIVE SUMMARY

The MARINE SCOUT Advancement project was undertaken to improve the formfactor and performance of the original MARINE SCOUT Unmanned Aerial System (UAS) payload. The original system was designed to operate with the PUMA UAS, an aircraft-style military drone with limited range and on-station capabilities. The MARINE SCOUT II payload was designed to operate on a quad or octocopter UAS system. The UAS selected was the Skyfront Perimeter 8, a commercial UAS system that is gas-powered and has a 3+ hour flight duration and 60+ mile range. The payload is designed to be weather and water-resistant (IP65) to allow long-duration, non-Visual Line-of-Sight (VLOS) flights in wide-ranging weather conditions to survey bodies of water for potential oil spills. The payload itself is a multispectral imaging system that collects Long-Wave Infrared (LWIR), Short-Wave Infrared (SWIR), Visible and Near-Infrared (VNIR), and Electro-Optical (EO) imagery and can download the imagery in real-time during flight to the MARINE SCOUT ground station.

The presence of an oil sheen on the surface of a body of water is detected using algorithms developed by Toomas Allik on two earlier projects for BSEE, MARINE SCOUT I (2018), and the Enhanced Oil Spill Detection project (2015). MARINE SCOUT II uses the same algorithms that use LWIR data and weather metadata to calculate an oil depth map for the scene. The oil detection algorithms can be run live on the MARINE SCOUT ground station to produce oil depth maps within seconds of the imagery being recorded. The payload is also capable of storing the imagery onboard even for long-duration flights if the downlink speed is degraded by distance or adverse flight conditions. The algorithms can then be run at the end of the flight. The resulting oil depth maps are tagged with the Global Positioning System (GPS) coordinates of the underlying images, which allows the resulting depth map to be loaded as an overlay on a Google Earth display of the terrain.

In addition to the LWIR-based oil depth map algorithms, MARINE SCOUT II developed water vs. terrain (declutter) algorithms that use the SWIR and VNIR data. The result of the declutter algorithm is a mask that can be used to constrain the oil depth algorithm. This way, the oil depth map is only calculated on the parts of images that contain water (or oil), which avoids any confusion in interpreting the final results.

Here is a summary of improvements made in MARINE SCOUT II:

- The payload was converted for use on commercial copter-style drones using commercial, open-frame gimbals.
- The payload was ruggedized (IP65) and made resistant to weather and moisture and can operate over a wide temperature range.
- The LWIR sensor was upgraded to include radiometric calibration and direct temperature measurement.
- A SWIR and VNIR declutter algorithm was developed to discern water from terrain.
- Situational awareness EO video was added.

- An inflight radio link was provided (WIFI 802.11 Wireless Ethernet and LTE 4G Cellular System) to allow payload control (C-and-C) and live imagery downloads.
- The algorithms were automated and streamlined to run in near-real-time on a full set of imagery and metadata.
- The resulting oil depth map can be loaded directly as a Keyhole Markup Language (KML) file into Google Earth.
- The ground station interfaces with a weather station so that weather metadata can be logged as part of flight collections.

As a result of these system advancements, the MARINE SCOUT II payload is suitable for field trials in remote or seaborne environments for long-duration, Non-Line-of-Sight (NLOS) flights. Additionally, the algorithms developed for this project are delivered in source code format to allow the customer to study and extend their functionality on MARINE SCOUT flight data or other BSEE data sets.

# Contents

List of Figures .....	ii
List of Tables .....	iii
<b>1 Abstract .....</b>	<b>4</b>
<b>2 Introduction .....</b>	<b>5</b>
<b>3 Review of Past Work.....</b>	<b>6</b>
3.1 Enhanced Oil Spill Detection Project.....	6
3.2 Remote Measurement of Thick Oil Spill Depth Using Thermal Imagery .....	8
3.3 MARINE SCOUT I.....	9
<b>4 Algorithm Design .....</b>	<b>12</b>
4.1 Oil Depth Daytime Algorithm .....	13
4.2 Oil Depth Nighttime Algorithm .....	16
4.3 SWIR/VNIR Declutter Algorithm.....	19
4.4 K-Means Clustering.....	20
4.5 Algorithm Flow .....	21
<b>5 MARINE SCOUT II .....</b>	<b>24</b>
5.1 System Design.....	25
<b>6 Flight Test.....</b>	<b>26</b>
6.1 CRREL.....	26
6.2 Flight Test Plan .....	28
6.3 CRREL Target Configuration .....	30
6.4 Results .....	31
6.4.1 Unknown Oil Depth Identification .....	31
6.4.2 Twilight Collection .....	33
6.4.3 Altitude Comparison .....	34
6.4.4 Water Temperature Determination .....	35
6.4.5 Confuser Identification and Masking.....	35
6.4.6 Water vs Terrain Identification .....	38
6.4.7 Sample Flight Test Results .....	39
<b>7 Conclusions.....</b>	<b>43</b>
<b>8 Future Work.....</b>	<b>44</b>
<b>9 References.....</b>	<b>45</b>
<b>10 Abbreviations and Acronyms .....</b>	<b>46</b>



## List of Figures

Fig. 1 Simultaneous visible and LWIR images of oil on water at Ohmsett.....	6
Fig. 2 Reflectivity spectra of ANS crude and its emulsified state.....	7
Fig. 3 Reflectivity spectra from five locations of tar emulsions from Santa Barbara channel, along with dead vegetation and reference standards .....	7
Fig. 4 Imagery from FLIR Systems T650sc LWIR camera (right) showed significant oil compared to visible imagery (left) .....	8
Fig. 5 The AeroVironment PUMA SUAS was selected for this program.....	9
Fig. 6. Calibrated LWIR thermal image .....	11
Fig. 7 MARINE SCOUT II algorithm flow.....	13
Fig. 8 Daytime heat transfer model .....	14
Fig. 9 Daytime oil thickness per pixel algorithm .....	14
Fig. 10 Oil depth map of target pool at CRREL .....	15
Fig. 11 Daytime oil depth map constrained to run over water/water-oil region-of-interest .....	16
Fig. 12 Thermal crossover of oil temperatures at night .....	17
Fig. 13 Nighttime heat transfer model .....	18
Fig. 14. Nighttime oil thickness per pixel algorithm .....	18
Fig. 15 Raw SWIR image of target pool and surrounding area at CRREL .....	19
Fig. 16 Oil depth map before and after using the SWIR-identified region of interest.....	20
Fig. 17 SWIR and LWIR CRREL images .....	21
Fig. 18 Clustered and co-registered SWIR image .....	22
Fig. 19 Final oil depth map .....	23
Fig. 20 MARINE SCOUT II payload showing FLIR LWIR sensor, SWIR sensor, and EO video.....	24
Fig. 21 MARINE SCOUT II payload showing side weather panel and top heat sink .....	25
Fig. 22 Airspace map of the CRREL location .....	26
Fig. 23 CRREL test pool location .....	27
Fig. 24 CRREL test pool at sunset showing oil targets and cover .....	28
Fig. 25 CRREL flight test – flight paths used for trials .....	30
Fig. 26 CRREL target pool configuration.....	30
Fig. 27 CRREL test pool with oil targets.....	31
Fig. 28 CRREL test conditions .....	31
Fig. 29 CRREL mystery oil depth results.....	32
Fig. 30 Ground truth vice calculated results .....	33
Fig. 31 CRREL sunrise and sunset algorithm results .....	34
Fig. 32 CRREL altitude sweep at 9:00 a.m. with moderate cloud cover.....	34
Fig. 33 CRREL water temperature determination (LWIR approach on the left, SWIR approach on the right) .....	35
Fig. 34 CRREL oil depth using different water temperature determination approach....	35
Fig. 35 CRREL LWIR image showing confuser target.....	36
Fig. 36 CRREL clustered SWIR image showing confuser clustered with terrain.....	37
Fig. 37 CRREL final oil depth map showing that confuser is masked out .....	37
Fig. 38 CRREL UAV launch site with pond nearby .....	38

Fig. 39 CRREL – Pond is detected as a region of interest by the SWIR clustering algorithm .....	38
Fig. 40 Flight #4 results .....	39
Fig. 41 Flight #7 results .....	40
Fig. 42 Flight #9 results .....	40
Fig. 43 Flight #12 results .....	41
Fig. 44 Flight #18 results .....	41
Fig. 45 Flight #20 results .....	42

## List of Tables

Table 1 Collection System Capabilities .....	10
Table 2 MARINE SCOUT II Flight Test Plan with Modifications .....	28
Table 3 CRREL Target Oil Thickness .....	31
Table 4 Specifications .....	43

# 1 Abstract

MARINE SCOUT Advancement is the second generation of the MARINE SCOUT payload. MARINE SCOUT stands for “mapping and reconnaissance imager, night-enhanced, for sensing of contaminants, oil, and unseen threats.” It is a multispectral optical collection system that can be mounted on a UAS. The original MARINE SCOUT payload was designed to fly on a PUMA UAS, which is a military fixed-wing drone. For MARINE SCOUT II, the payload was converted for use with commercial, multi-rotor, copter-style drones, specifically the Skyfront Perimeter 8 drone. The P8 is gas-powered and has superior range (60+ miles) and duration (3+ hours), and its avionics allow it to fly hands-off in non-VLOS conditions.

The purpose of the Advancement effort is to improve the payload to make it suitable for real-world data collections – flying over bodies of water, lakes, rivers, or oceans, scanning to find oil spills. To make the payload more suitable, the thermal sensor was improved, and the payload was ruggedized and made weather and moisture resistant, capable of flying long-duration flights over wide temperature ranges. Further, the communications were improved to allow downloading imagery live during flight when the downlink quality is sufficient and use a store and forward approach if the bandwidth is low or nonexistent. The algorithms, which run on the system ground station, were automated and streamlined so that a set of images (LWIR, SWIR, Near-Infrared (NIR)) and metadata (altitude, GPS, weather data) can be processed in only a few seconds.

The oil detection algorithms, both daytime and nighttime variants, are reused in principle from the initial MARINE SCOUT development. They were rewritten for MARINE SCOUT II but using the detailed formula descriptions from Toomas Allik’s early published papers. The operation of the oil depth (heat map) algorithm is based on the underlying effect that an oil sheen on the surface of a body of water absorbs the solar loading more than the water and thus heats up compared to the water. The thicker the oil sheen, the more it heats up. This effect is meaningful when running the algorithm on an image that is covered by water or a water-oil mix, but it is not meaningful when looking at terrain or waterborne confusers such as seaweed. Therefore, on MARINE SCOUT II, we used the SWIR and VNIR imagery to create a mask identifying the water/water-oil regions of the imagery, so that we could constrain the oil depth algorithm to run on those relevant regions (i.e., where its oil depth results would make sense). The SWIR/VNIR algorithm and the clustering algorithm were developed and optimized on this project.

At the end of the project, the payload and algorithms were subjected to a rigorous flight test at the Army’s Cold Regions Research and Engineering Laboratory (CRREL) in Hanover, NH. The results obtained are detailed in Section 6, Flight Test, of this report.

## 2 Introduction

The MARINE SCOUT Advancement project is the latest in a series of studies and sensor developments designed to remotely detect the presence of oil spills in bodies of water. In 2015, Toomas Allik studied various types of sensors – LWIR, SWIR, NIR – for their suitability of detecting oil sheens in Degraded Visual Environments (DVE). He found that LWIR thermal imagery was the most suitable way to detect oil sheens in low-light environments. Furthermore, he found that it was the most reliable in higher light conditions as well. The original MARINE SCOUT project intended to exploit the earlier findings by developing an airborne payload with sensors for LWIR light (8 to 12  $\mu\text{m}$ ), SWIR light (1 to 2.5  $\mu\text{m}$ ), and NIR light (0.4 to 0.9  $\mu\text{m}$ ). While the payload was designed to be mounted and flown on a PUMA UAS, the inflight conditions for the optics were very challenging, and the final data collections were performed with the payload mounted to a crane at BSEE’s Ohmsett facility. The data collected was analyzed post-collection using an oil heat map algorithm based on the LWIR data. Previously oil spills have been detected using a similar approach, but in MARINE SCOUT, the goal was to use the heat map to predict the depth of oil in the sheen. This was found to be effective.

For the MARINE SCOUT Advancement project, or MARINE SCOUT II, the primary purpose was to repackage the payload for use in actual field environments using a commercial multi-rotor drone and open-frame gimbal. Also, the LWIR sensor was upgraded to a radiometrically calibrated, more modern design that could read the pixel temperatures right from the collected imagery. For comms, the payload was equipped with a radio interface capable of downloading captured imagery in real-time if the drone was in Line of Sight (LOS) and the prevailing conditions were amenable, and the algorithms were streamlined to run on the ground station with near real-time responsiveness. All of these improvements were designed to allow the payload to fly for field tests in real-world environments (i.e., Alaska, Gulf of Mexico). The oil depth algorithm for day and night conditions were the same as in the previous MARINE SCOUT project, but declutter algorithms were also developed using SWIR or VNIR imagery, and clustering was used to create a mask for each set of images to bound the portion of the image that contains either water or a water/oil mix.

### 3 Review of Past Work

#### 3.1 Enhanced Oil Spill Detection Project

In 2015, Toomas Allik [Allik, 2015] undertook a study for BSEE in Enhanced Oil Spill Detection Sensors in Low-Light Environments. In the study, he analyzed images taken by various kinds of sensors in low-light conditions to see which, if any, detected the presence the oil sheen on the water. He was primarily interested in low-light or DVE. He was looking at infrared bands, LWIR, MWIR, SWIR, and NIR, and noticed that SWIR and LWIR radiation was present at night (i.e., night glow, thermal emissions), and might provide better imagery to detect oil spills in DVE conditions. He also noticed that water has an absorption band in the infrared range, so subsurface features in the water were occluded but surface contrast for oil vs. water areas were potentially useful. In non-night DVE conditions (i.e., fog or rain), the NIR, SWIR, and Mid-Wave Infrared (MWIR) bands attenuated badly, and LWIR imagery was generally much better.

For oil detection, Allik noted that LWIR images were able to visualize oil spills on calm and agitated water (**Fig. 1**).

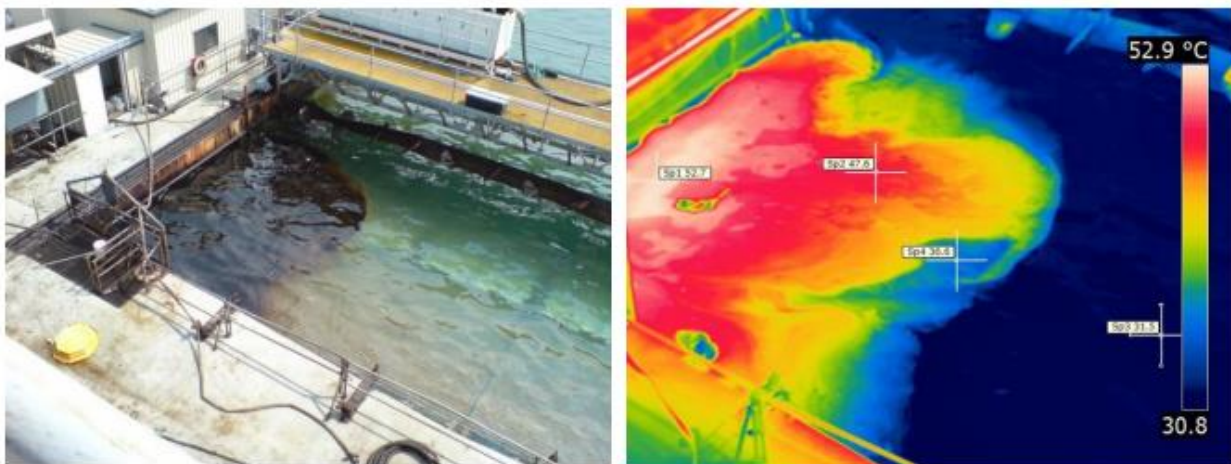


**Fig. 1 Simultaneous visible and LWIR images of oil on water at Ohmsett**  
(Photo: Toomas Allik, 2018)

He also studied the reflectance of oil spills of different thicknesses in the NIR and SWIR bands and found that crude and crude-emulsions behaved differently, and that different types of crude emulsified at drastically different rates in the field (**Fig. 2**).

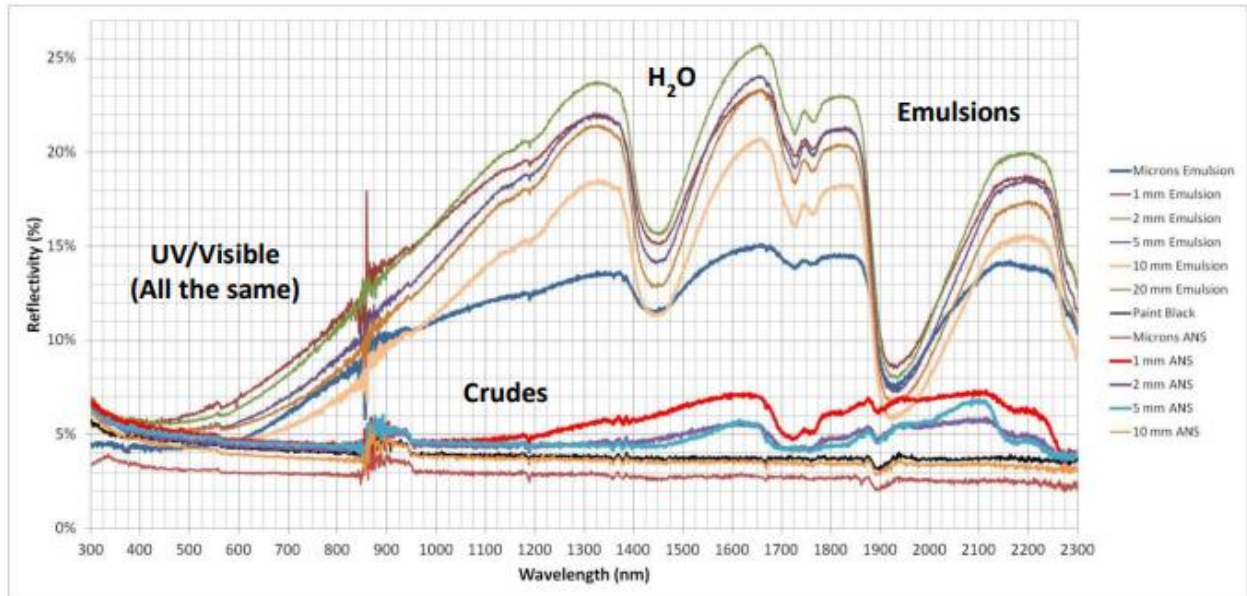


**Fig. 2 Reflectivity spectra of ANS crude and its emulsified state**  
 (Photo: Toomas Allik, Figure 13, 2018)

To trial-test whether SWIR imagery can be used to determine oil thickness, data was collected at natural oil seeps near Santa Barbara, CA. Since oil has some spectral absorption bands in the SWIR wavelength ranges, the approach was to compare the two wavelengths (1.2 $\mu$ m and 1.25 $\mu$ m). He found the reflectivities in **Fig. 3** from several sites along with significant interference from vegetations (sea kelp).

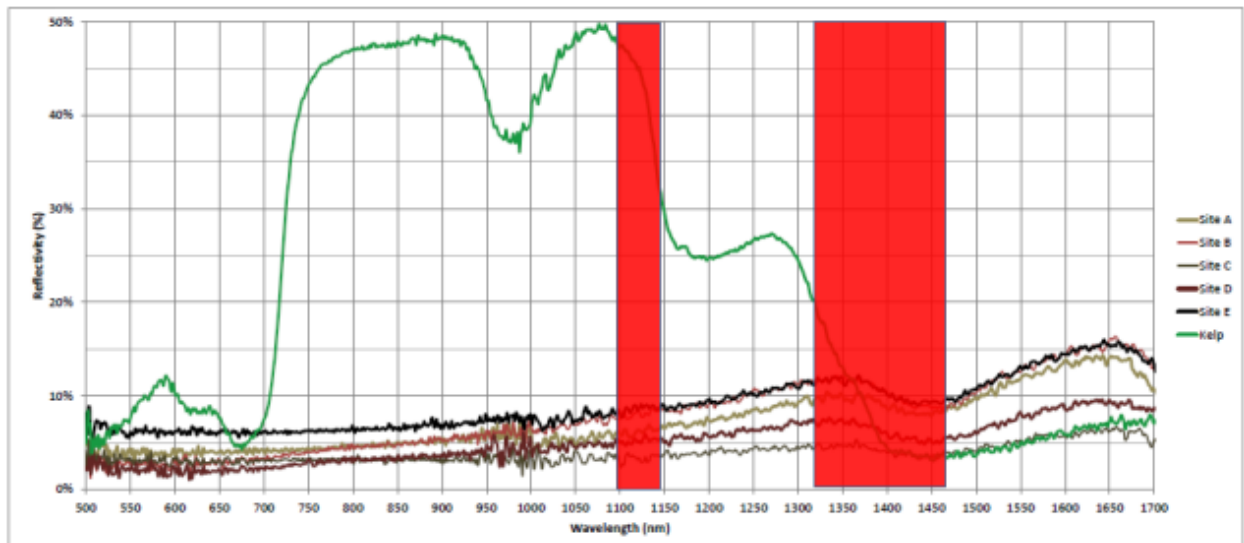


**Fig. 3 Reflectivity spectra from five locations of tar emulsions from Santa Barbara channel, along with dead vegetation and reference standards**  
 (Photo: Toomas Allik, Figure 25, 2018)

A later collection in Santa Barbara was analyzed and reviewed for thermal signatures (LWIR) and was able to identify significant amounts of oil in the seep locations. The imagery was recorded in the early morning crossover time, so it would have been even better at other times of the day (**Fig. 4**).



**Fig. 4 Imagery from FLIR Systems T650sc LWIR camera (right) showed significant oil compared to visible imagery (left)**

(Photo: Toomas Allik, Figure 36, 2018)

The conclusion to this early study was that LWIR was a good and low-cost method to detect oil spills for crude and emulsified oil for thick spills, and that SWIR methods for spill detection and clutter rejection were promising, particularly for weathered emulsions, but needed more evaluation. He recommended creating a spectral database for various types of crude oils and weathered emulsions and suggested more studies to establish methods to determine ground truth and data calibrations.

### **3.2 Remote Measurement of Thick Oil Spill Depth Using Thermal Imagery**

In 2018, Toomas Allik [Allik, 2018] published a study with BSEE that focused on using LWIR (thermal) imagery to determine oil depth in thick oil spills. This was a continuation of work from his earlier study and used a Forward-Looking Infrared (FLIR) T640SC camera to record imagery every 15 minutes for 24 hours of Alaska North Slope (ANS) crude in both crude and emulsified formats. He created a daytime and nighttime heat transfer model that was able to calculate the oil thickness within one or two standard deviations. The issue that he was trying to address was to create the capability to remotely detect and measure oil spills that can be used any time (around the clock and in DVE environments) and can provide its quantitative analysis quickly.

Allik's heat transfer model included terms for radiation, convection, and conduction. It is able to calculate oil thickness by measuring the oil surface temperature, air and water temperature, solar radiation, and wind speed. The night calculation includes radiation cooling, cloud cover percentage, and humidity. Both models should work at a basic level of accuracy.

The daytime heat transfer model was computed to be shown below, where  $L$  is the thickness of the oil sheen.

$$L = \frac{k_o (T_o - T_w)}{\text{Solar Radiation} - \varepsilon\sigma(T_o^4 - T_a^4) - h_o (T_o - T_a)}$$

The model was tested at BSEE's Ohmsett test facility in New Jersey and show good correspondence between computed values for the thickness and the actual thickness of the oil in the samples. There is some variance between different types of oil.

For the nighttime heat transfer model, the solar radiation value is zeroed out, and the Swinbank downward thermal night sky radiation is included (i.e., includes cloud cover and ceiling data). This gives the following relation.

$$L = \frac{k_o (T_w - T_o)}{\varepsilon\sigma(T_o^4) - [(1 + KC^2) \times 8.78 \times 10^{-13} \times T_a^{5.852} \times RH^{0.07195}] + h_o (T_o - T_a)}$$

During the day, thicker oils get hotter than thinner ones, but at night this relation is reversed. The heat transfer model was able to compute the oil thickness with reasonable accuracy.

These models were used in the MARINE SCOUT Advancement project.

### 3.3 MARINE SCOUT I

In MARINE SCOUT I, QinetiQ worked with BSEE to design and build a multi-spectral payload that could fly on the AeroVironment PUMA Soldier Unmanned Aircraft System (SUAS) platform. The PUMA is a fixed-wing style drone (**Fig. 5**).



**Fig. 5 The AeroVironment PUMA SUAS was selected for this program**

(Photo: Scot Myhr, et al., Figure 1, 2018)

The system operated in two modes: reconnaissance mode and Full Motion Video (FMV) mode. The video mode is for situational awareness. Spectral data is only collected in reconnaissance mode. The payload collected LWIR, SWIR, and NIR imagery. Since the payload was designed



for fixed-wing Unmanned Aerial Vehicles (UAVs), algorithms were incorporated to compensate for forward motion and the rotational effects of the flight to allow imagery to be mosaiced in a precise and repeatable way.

The collection system capabilities are encapsulated in **Table 1**.

<b>Table 1 Collection System Capabilities</b>	
<b>Enhancement</b>	<b>Airborne Payload</b>
Forward Motion Compensation and Pointing	Linear stage eliminates image smearing for improved resolution in mapping the water/land. Rotary stage compensates image skew due to yaw-angle effects (platform crabbing) at nadir. Outer gimbal maintains nadir or off-nadir LOS pointing in presence of platform roll.
High-Fidelity Multispectral Digital Sensors	True day/night capability using high-dynamic range digital uncooled thermal infrared camera. Dual-band NIR-SWIR using high-dynamic range digital InGaAs sensor and filter paddle. Custom optics providing high throughput, wide Field of View (FOV), and low distortion over the full FOV.
Enhanced Digital Data Link (DDL)	Digital imagery transmission improves resolution, dynamic range, and sensitivity vs. analog. Tailored DDL link can simultaneously transmit digital imagery and FMV.
Onboard Native Data Storage	Real-time, lossless storage of digital imagery robustly accommodates communication issues (e.g., unpredictable performance in the DDL) using a store-and-forward paradigm.
Enhancement	Ground station.
Quasi-Radiometric Calibration	Sensors are not radiometrically calibrated, so software performs an in-scene projection using water temperature estimation and other sources, when available (e.g., test blackbodies).
Visualization and Manipulation	Display, manipulate, and compare multi-spectral/multi-pass mosaics. Generate reports for forensics, analysis.

The results for a data collection are shown in **Fig. 6**.

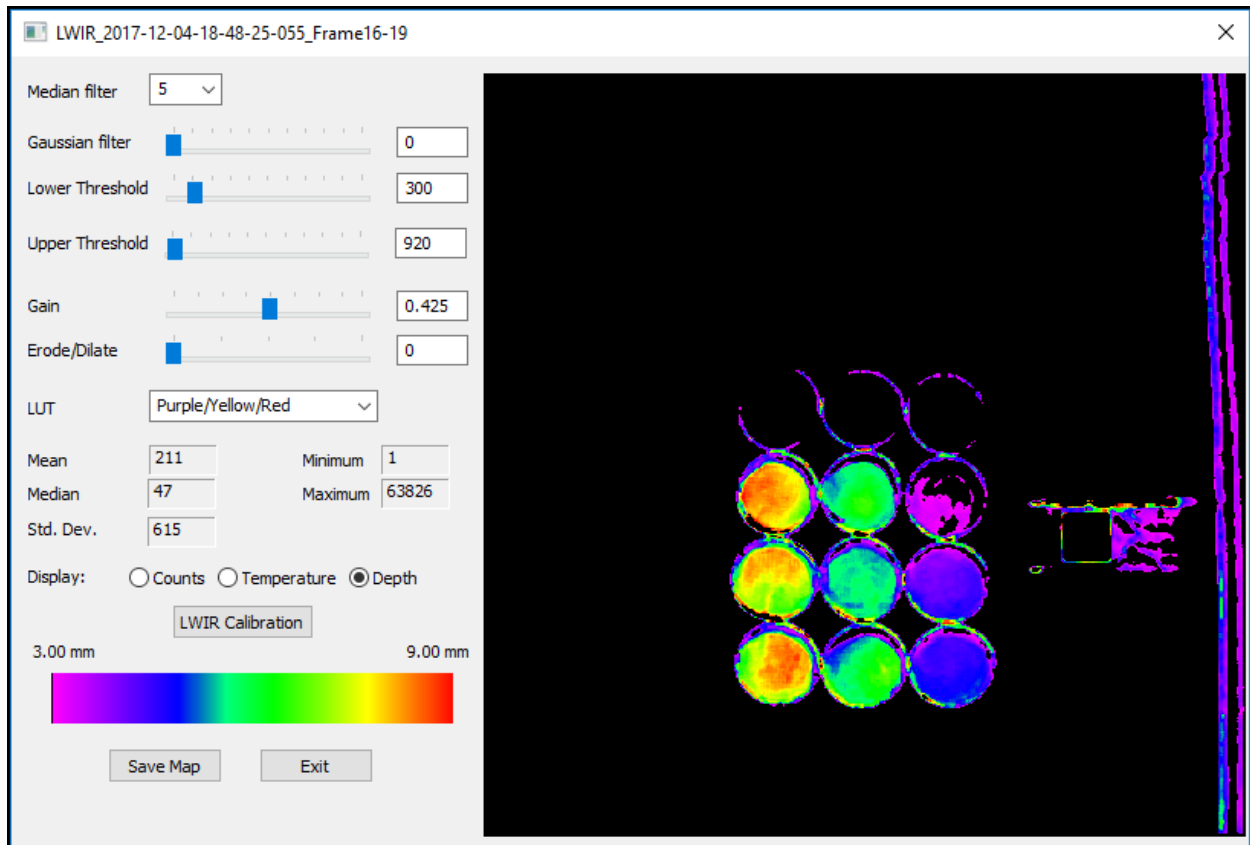


**Fig. 6. Calibrated LWIR thermal image**  
 (Photo: Scot Myhr, et al., Figure 10, 2018)

SWIR and NIR imagery were used experimentally to reject clutter in the imagery. These algorithms were not used on the MARINE SCOUT Advancement project.

## 4 Algorithm Design

The MARINE SCOUT Advancement project was undertaken primarily to convert the payload into a rugged, deployable configuration designed for use with long-haul, quad, or octocopter UAS systems. The initial plan was to reuse all the algorithms previously developed by Toomas Allik in the earlier projects and to convert them for use in a near-real-time context. In MARINE SCOUT I, the imagery that was collected on a flight was consolidated post-flight and sent to a remote analyst for processing. The resulting heat maps were then provided back to the field team the next day, compromising the effectiveness of the system to be used operationally. MARINE SCOUT II intended to address that issue by streamlining the existing algorithms and converting them to run automatically without needing an analyst in the loop. Also, the downlink pathway between the payload and operator ground station was enhanced (WIFI and LTE links available simultaneously) to allow spectral imagery and situational awareness video to be streamed to the ground station live during collections. This allows the ground station to keep up with the flow of imagery from the payload, both from a storage standpoint and an algorithm execution standpoint.

For the purposes of flight testing, the payload was typically flown at 200' Above Sea Level (ASL), and imagery was collected every 6 seconds from all spectral optics. The imagery is then downloaded to the ground station if the downlink is of sufficient quality or stored onboard until the downlink has the bandwidth available to send the imagery. When the imagery is available on the ground station, the FLIR camera's meta-data is extracted (GPS data and altitude), and the images are matched up to the current weather meta-data to provide the oil depth algorithms with all the information needed to create the heat maps.

For the MARINE SCOUT Advancement project, it was discovered that the original source code for the algorithms created by Toomas Allik was no longer available. However, the daytime and nighttime heat transfer algorithms were well documented in the papers cited in earlier sections, so they were easily re-created from scratch. The declutter algorithms using the SWIR and VNIR images were not described in sufficient detail to allow them to be re-created from scratch, so the algorithm team set out to design and optimize the declutter algorithms from scratch for the project. The basic flow of the algorithms is shown in **Fig. 7**, but the concept is that LWIR, SWIR, and VNIR images are all recorded simultaneously. The SWIR image is analyzed to determine if it is usable (i.e., neither over- nor under-saturated). If it is usable, the LWIR and SWIR images are co-registered to precisely overlap the images. This is needed because, although bore-sighted, the sensors have non-identical FOVs. Then the SWIR image data is used to determine the regions of interest (i.e., water and water mixed with oil areas) and exclude terrain features and waterborne confusers such as seaweed or other vegetative debris. The co-registered mask is then passed to the oil depth algorithm, which is then constrained to run over the regions of interest. The daytime algorithm uses LWIR data where the temperature value can be read off for each pixel, payload metadata (i.e., GPS, altitude), and weather metadata (i.e., solar load, air temperature, wind speed). The water temperature is determined from the LWIR data. The resulting heat map can be overlaid either on the existing imagery or onto a Google Earth map for display purposes.

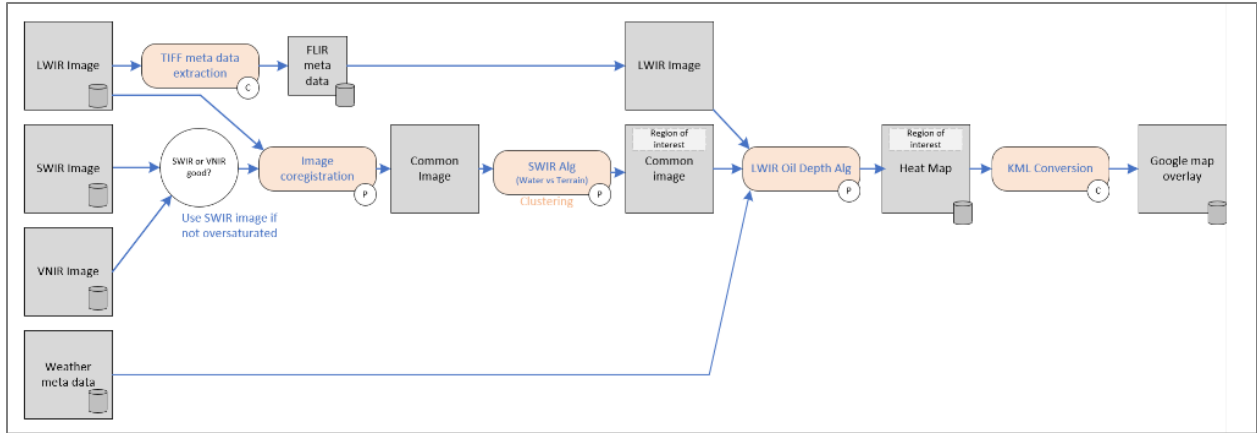


**Fig. 7 MARINE SCOUT II algorithm flow**

If the SWIR image is not usable in the first step, the VNIR image is checked for usability, and the same process is followed. If neither is usable – which typically happens in heavy overcast, rainy, or twilight/dark conditions – the oil depth algorithm is run against the entire image. The resulting depth map is accurate for the oil sheen areas of the images, but since the declutter mask can't be used, the oil map contains a lot of areas that are not relevant.

#### 4.1 Oil Depth Daytime Algorithm

The daytime heat transfer algorithm was developed and formalized by Allik, 2018. It is based on the idea that thick oil sheens will absorb more solar radiation than the surrounding water and will have a proportionally higher temperature depending on the thickness of the oil. There is a slight dependency on the type of oil (i.e., ANS vs. Hoover Offshore Oil Pipeline System (HOOPS)), but all of them show this same effect. The solar radiation heats up the oil while convection, conduction, and radiation all work to dissipate the heat (**Fig. 8**).

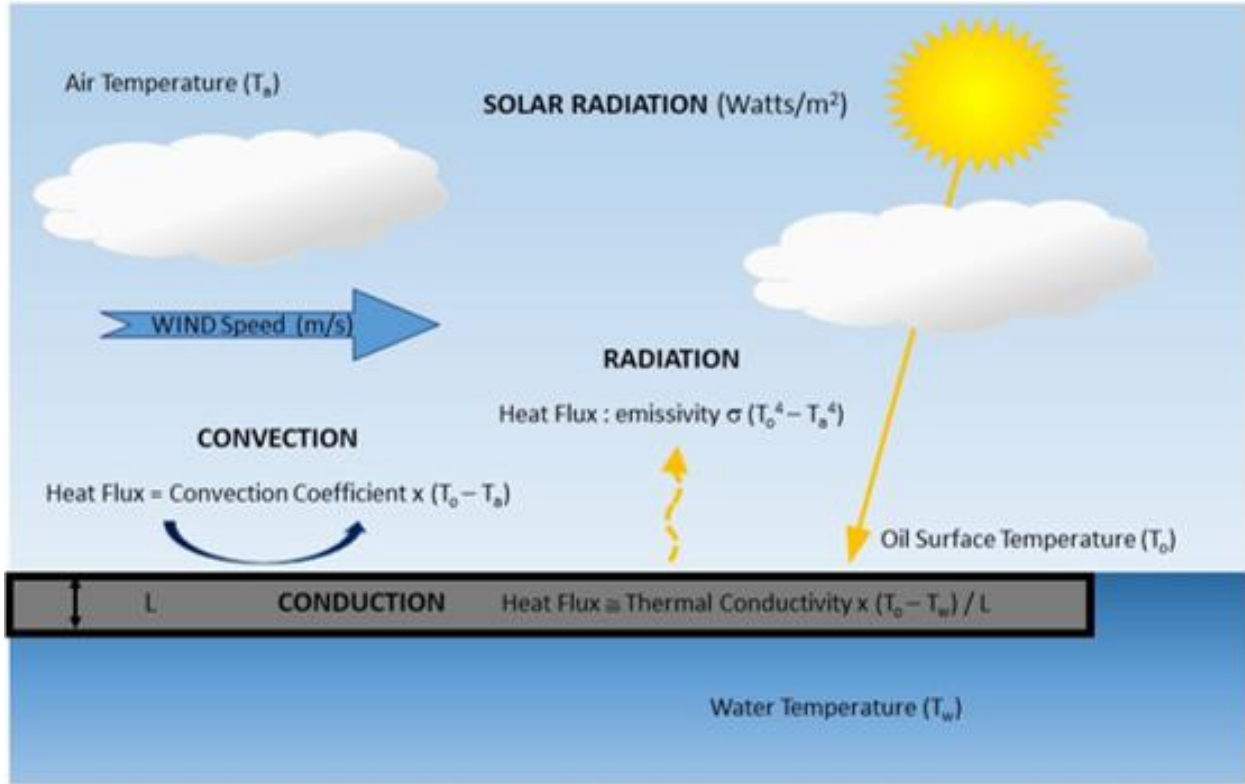


**Fig. 8 Daytime heat transfer model**  
(Photo: Toomas Allik, 2018)

**Fig. 9** shows the consolidated formulas for the depth map algorithm.

**SOLAR RADIATION = CONDUCTION + CONVECTION + RADIATION**

Fourier's Law	Thermal Conductivity $(T_o - T_w)/L$
Newton's Law of Cooling	Air Convection Coefficient $(T_o - T_a)$
Stefan-Boltzmann Law	Oil Emissivity $(5.67 \times 10^{-8} \text{ W/m}^2\text{K}^4) (T_o^4 - T_a^4)$

$k = 0.126 \text{ W/m(K)}$

**Oil Thickness L (mm) =**  $\frac{1000 \times \text{Thermal Conductivity} \times (T_o - T_w)}{\text{Solar Radiation} - \epsilon\sigma(T_o^4 - T_a^4) - \text{Air Convection Coefficient} (T_o - T_a)}$

**Fig. 9 Daytime oil thickness per pixel algorithm**  
(Photo: Toomas Allik, 2018)

**Fig. 10** shows a sample of the oil depth map algorithm running on an LWIR image collected at CRREL. The image was collected at sunset, so the SWIR image was not suitable for identifying the target pool region of interest, so the algorithm was run over the entire image. For practical purposes, the image is difficult to interpret even though it can discriminate the presence of the oil because there are other areas in the image that are higher temperature regions that could be confused for an oil sheen but aren't.

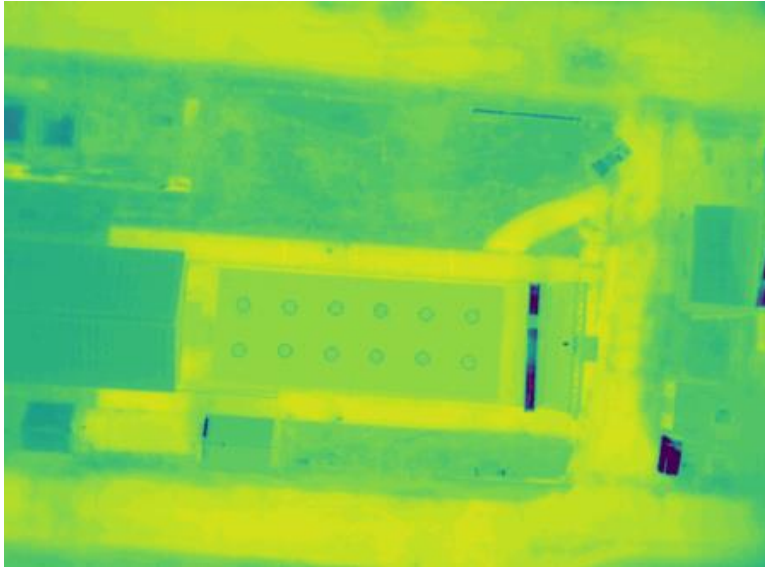


**Fig. 10** Oil depth map of target pool at CRREL

If the SWIR image can be used to identify regions of interest, then the resulting oil depth map will only run over the regions of interest and create a more relevant result (**Fig. 11**).

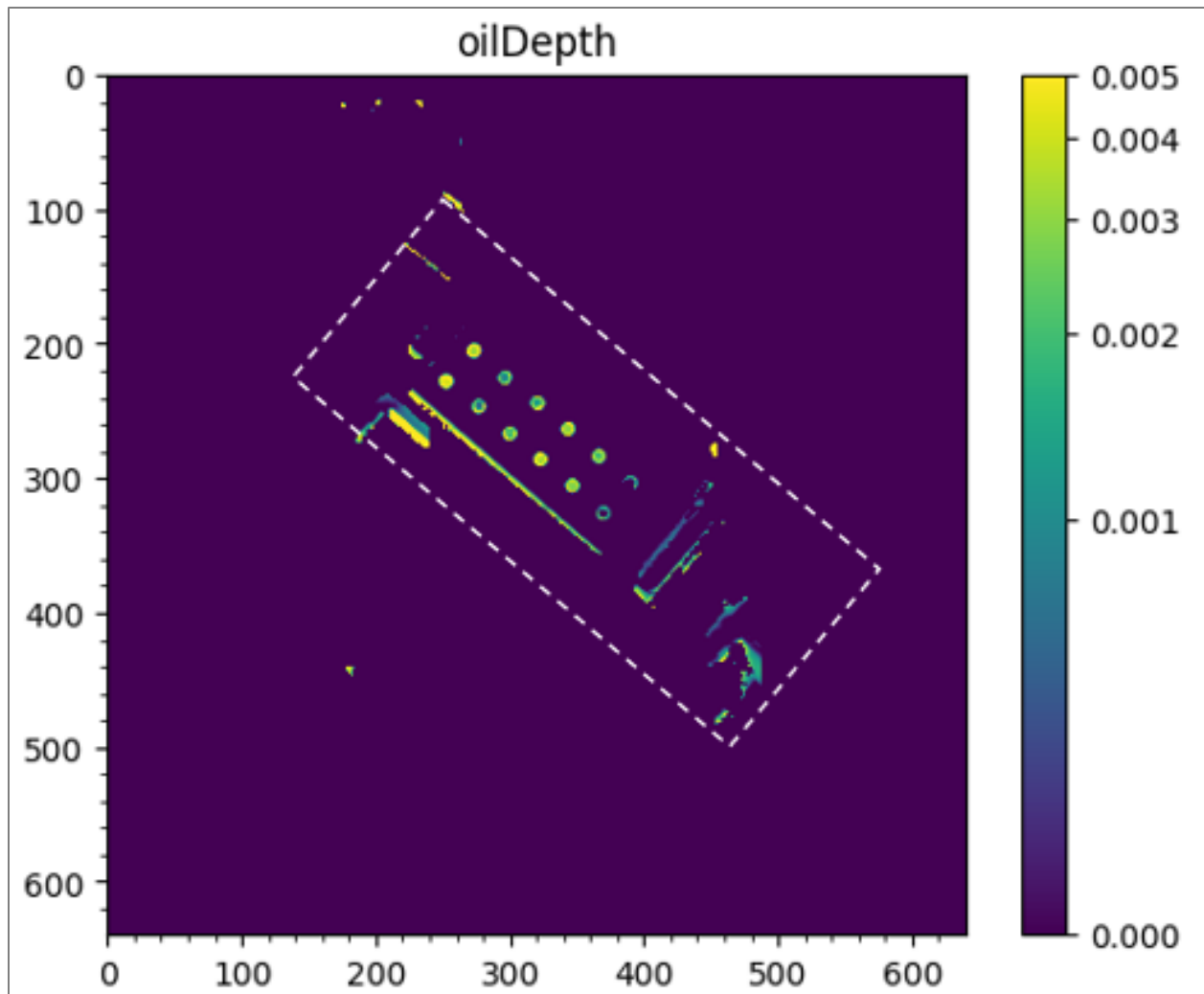
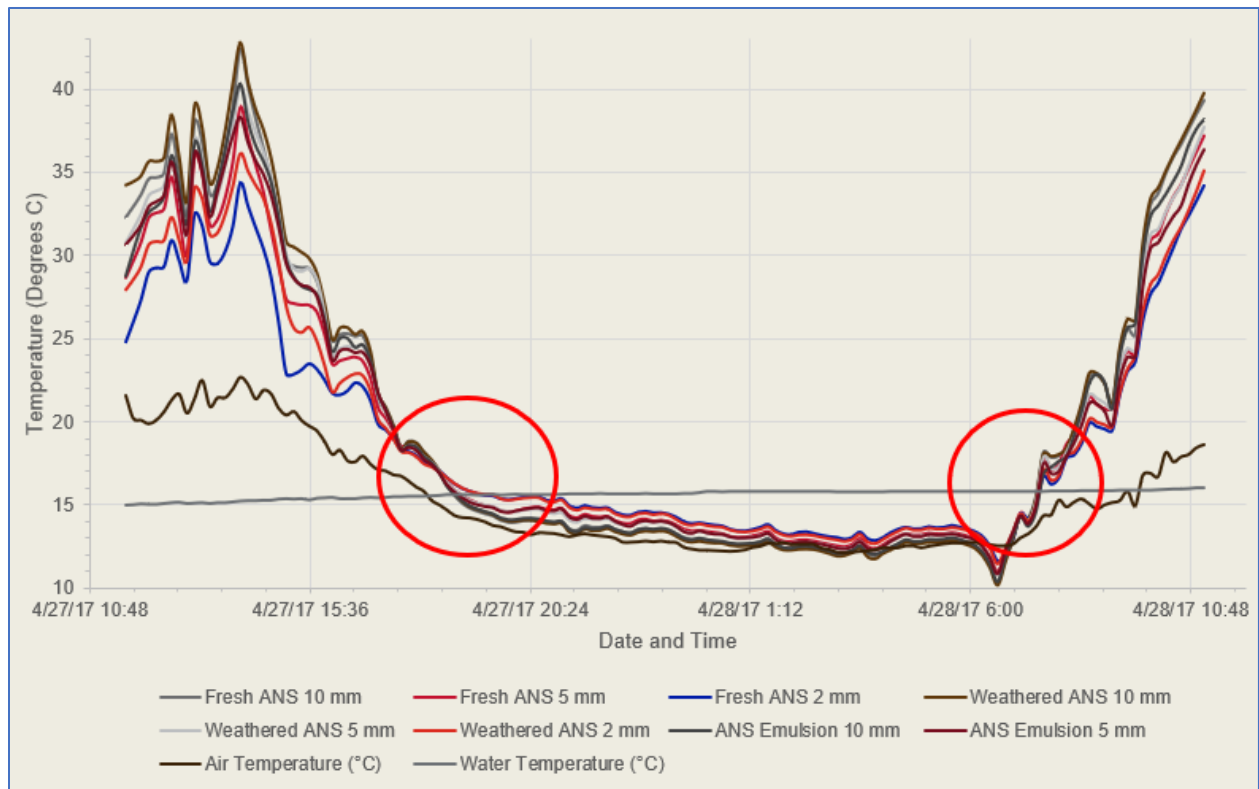


Fig. 11 Daytime oil depth map constrained to run over water/water-oil region-of-interest

## 4.2 Oil Depth Nighttime Algorithm

The nighttime heat transfer model was also developed in 2018 [Allik]. It is based on oil sheens cooling more rapidly than the surrounding water once the solar loading is removed. The effect shown in **Fig. 12** was developed in 2018 [Allik].



**Fig. 12 Thermal crossover of oil temperatures at night**  
 (Photo: Toomas Allik, 2018)

At night, the heat within the oil sheen is dissipated due to convection, radiation, and night radiative cooling (**Fig. 13**).



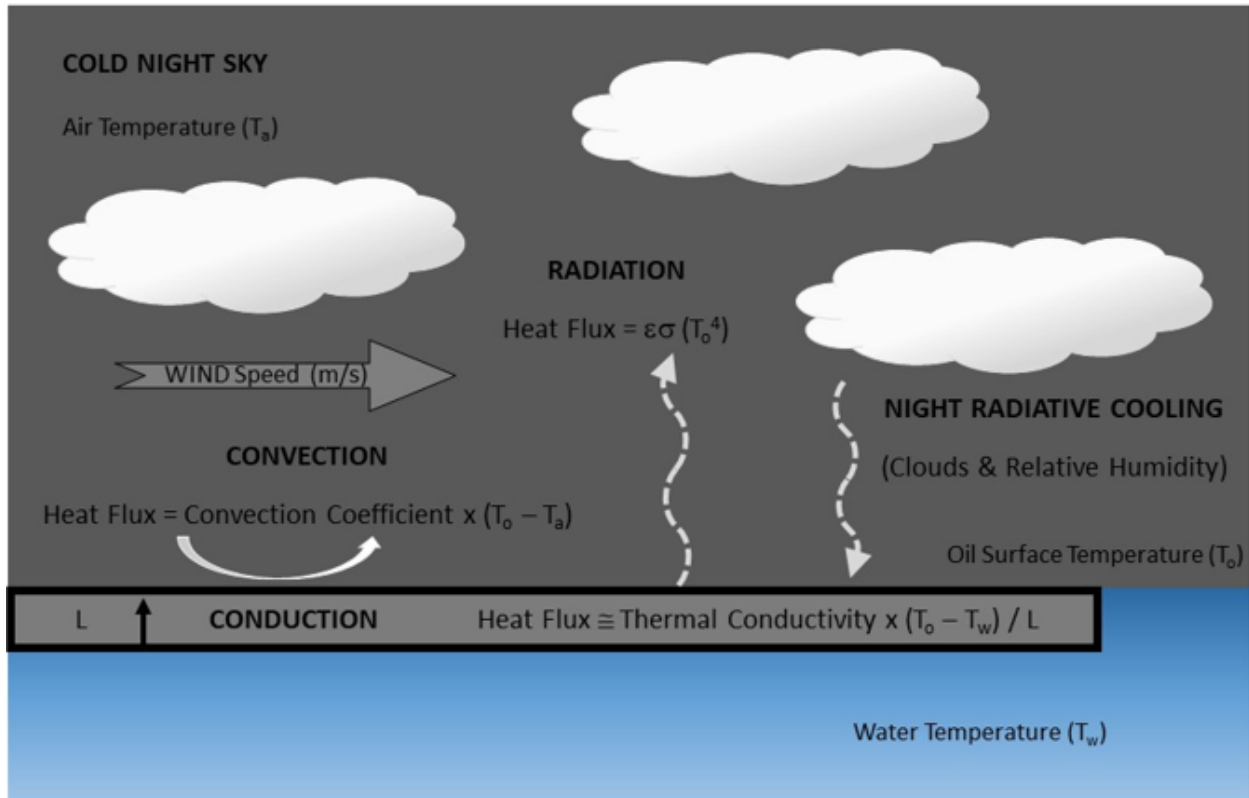


**Fig. 13 Nighttime heat transfer model**

The resulting oil depth map formula to compute the oil thickness is shown in **Fig. 14**.

$$\text{Oil Thickness (mm)} = \frac{1000 \times \text{Thermal Conductivity} \times (T_w - T_o)}{\epsilon \sigma (T_o^4) - \left[ (1 + KC^2) \times 8.78 \times 10^{-13} \times T_a^{5.852} \times (\text{Relative Humidity \%})^{0.07195} \right] + \text{Convection Coefficient} (T_o - T_a)}$$

**Fig. 14. Nighttime oil thickness per pixel algorithm**

(Photo: Toomas Allik, 2018)

Since the SWIR images will not be usable at night, the depth map algorithm will be run over the entire LWIR image. The LWIR image is used to determine the temperature (of each pixel) as well as the water temperature. Additional factors used are provided by the weather station and are the air temperature, percent cloud cover, wind speed, and relative humidity.

During testing, we used the nighttime model any time the solar radiation load fell to zero (rain, heavy overcast, early morning, sunset, and during twilight conditions). We found that the images showed flattened depths where the variance of calculated oil depths was less than the known oil depths in the targets.

### 4.3 SWIR/VNIR Declutter Algorithm

Initially, we planned to use differences between the SWIR imagery and the VNIR imagery to identify water and water/oil regions in the co-registered imagery. This was based on Toomas Allik's findings that oil had different spectral performance in the SWIR and VNIR spectral bands. However, we found early on that the water and water/oil regions of "good" SWIR images showed similar intensity levels for the water and water/oil regions and a variety of levels for terrain or waterborne confusers (**Fig. 15**).



**Fig. 15** Raw SWIR image of target pool and surrounding area at CRREL

In Fig. 15, all the water and water/oil areas are in the target pool and have very similar intensities, while the non-watery areas vary considerably. We determined that a clustering algorithm, 3-segment K-Means clustering in this case, would work well to aggregate all the water and water/oil areas into one region while excluding the bulk of everything else. We found that this approach worked very well when flying over mixed terrain (**Fig. 16**).

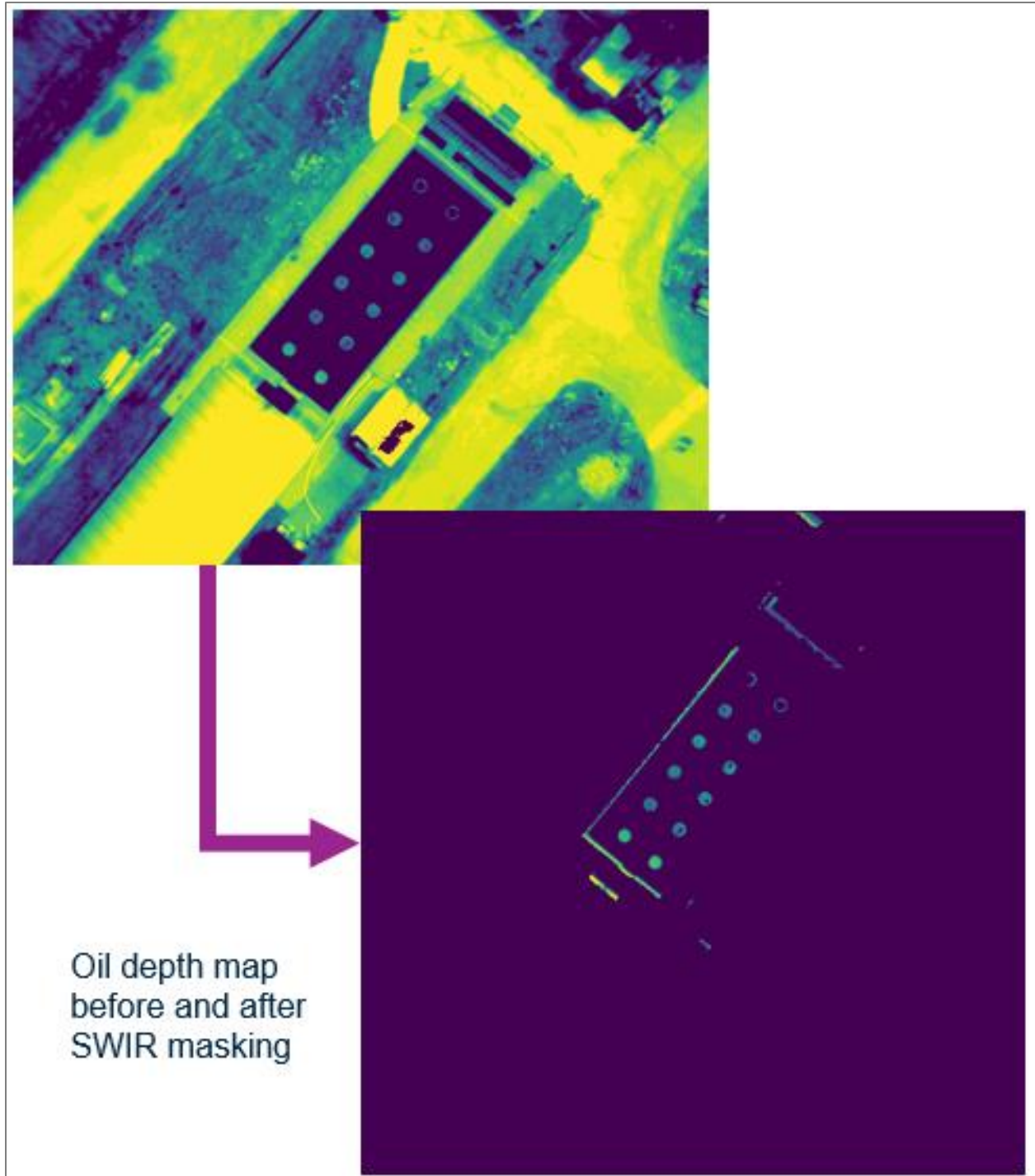


Fig. 16 Oil depth map before and after using the SWIR-identified region of interest

#### 4.4 K-Means Clustering

For MARINE SCOUT II, we added the use of a 3-segment, K-Means clustering algorithm to create the constraint mask for the oil depth algorithms. When the SWIR or VNIR images were suitable, the approach worked well to identify the water and water/oil regions and cluster them

into region(s) of interest. In the event that the SWIR and VNIR images were over- or under-saturated (typically in low-light conditions), we ran the K-Means algorithm on the LWIR images to attempt to identify the water region(s) of interest, which is needed to get the temperature of the water for the depth algorithm. We found that it worked decently well to identify an area to use to determine the water temperature, but not that well to identify the whole region of interest in the LWIR imagery.

K-Means clustering generally works well with SWIR images that are taken in good lighting scenarios. Sometimes it captures other parts of the image into the region(s) of interest, but generally aggregates the water and water/oil areas very well. Even if some small portion on non-water areas are captured, the overall level of clutter is drastically reduced, making the resulting oil depth map much easier to interpret.

#### 4.5 Algorithm Flow

The payload takes LWIR, SWIR, and VNIR images as close to simultaneously as possible. If the SWIR image is good (i.e., not over- or under-saturated), it is used. Otherwise, the VNIR image is checked. In good light conditions, the SWIR image is generally of sufficient quality. **Fig. 17** shows samples of corresponding SWIR and LWIR images of the test pool at CRREL.

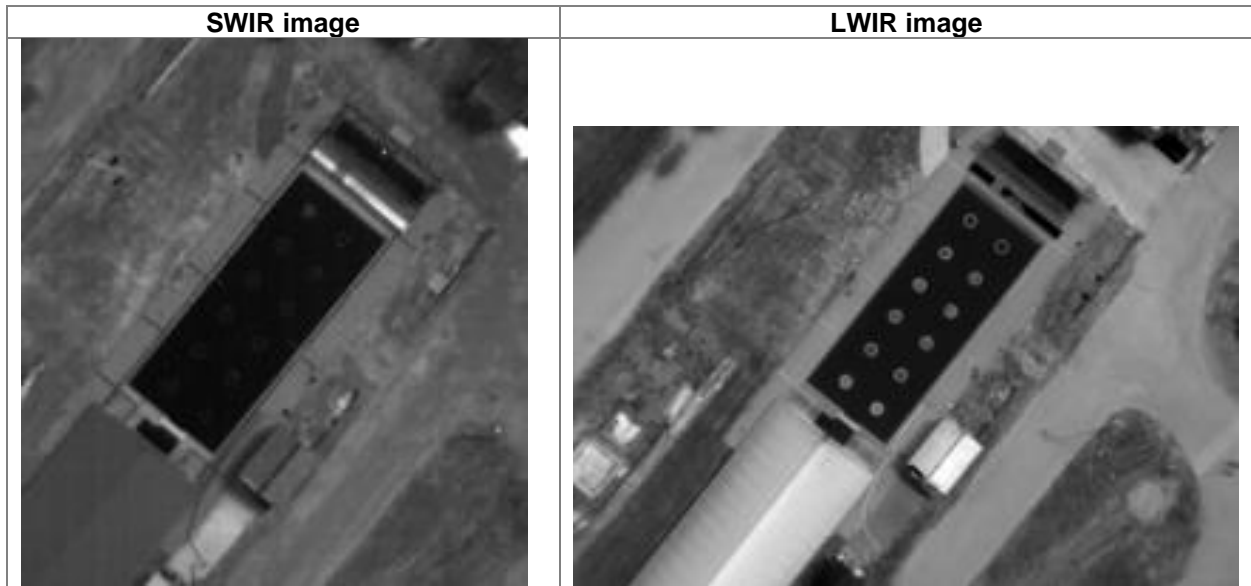


**Fig. 17 SWIR and LWIR CRREL images**

The images in Fig. 17 are co-registered, and the SWIR image is clustered using the K-Means algorithm. This results in a constraint mask for the LWIR oil depth algorithm. The co-registered and clustered SWIR image is shown in **Fig. 18**.

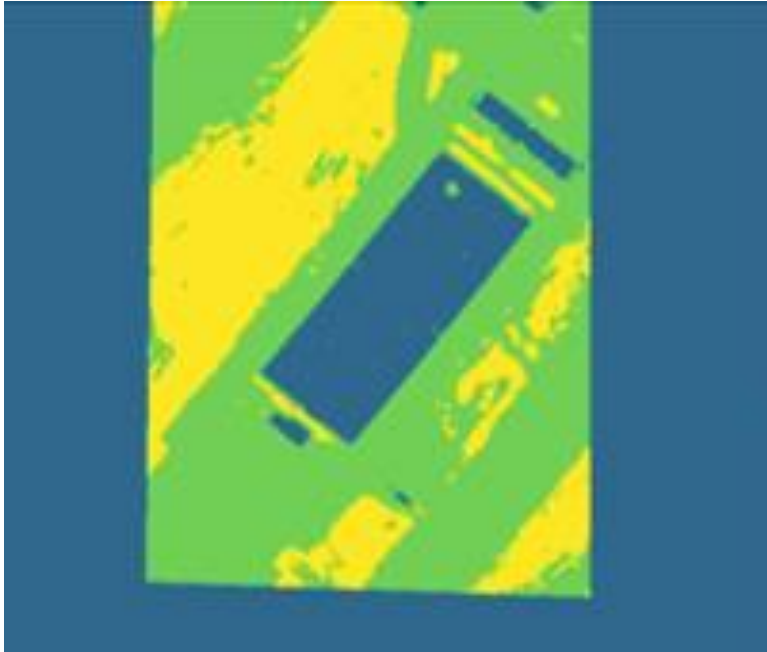


**Fig. 18 Clustered and co-registered SWIR image**

The daytime oil depth algorithm is then run using the constraint mask to produce the scene's oil heat map (**Fig. 19**).

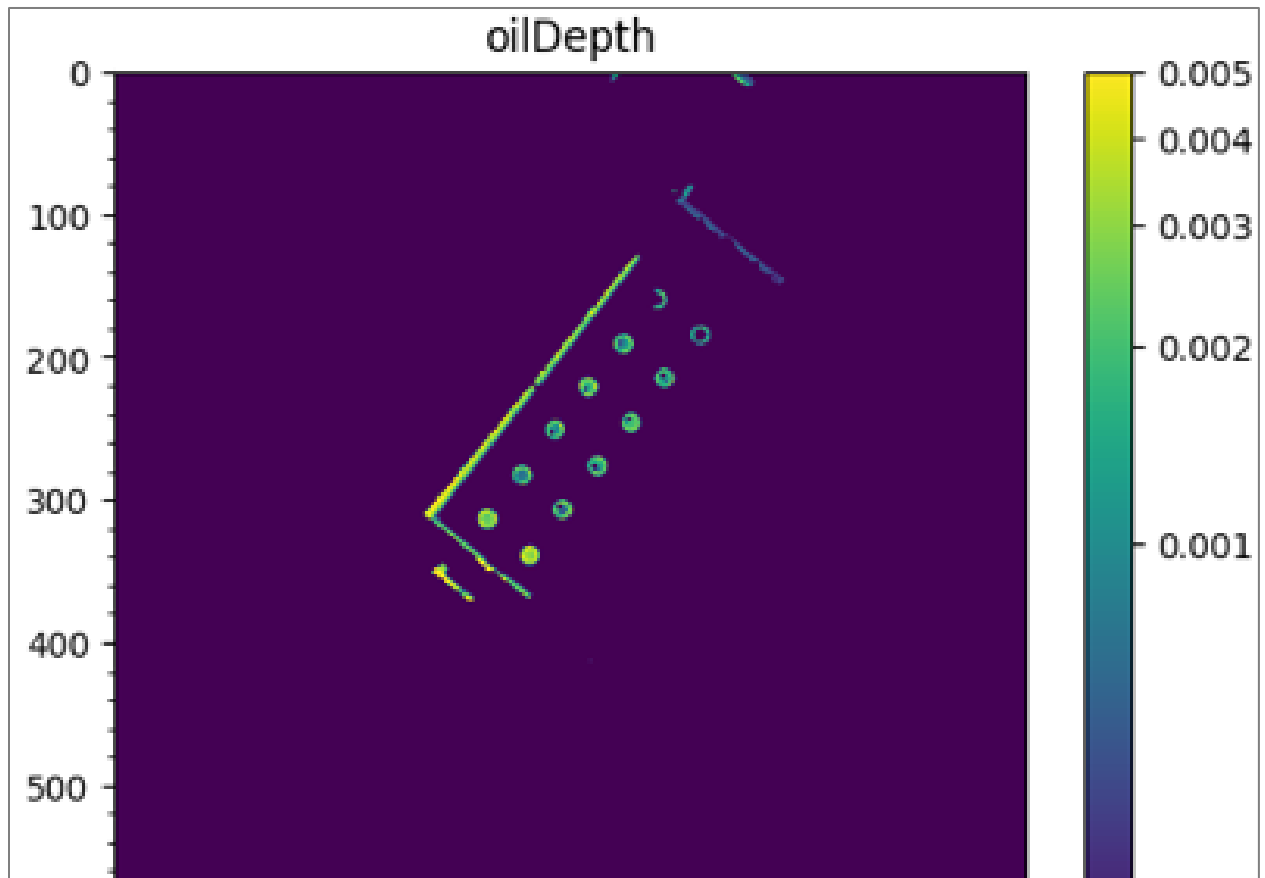


**Fig. 19 Final oil depth map**

In Fig. 19, the CRREL target pool is readily discernable with the warmer oil targets showing clearly. Note that the oil depth increases towards the bottom, hence the higher temperatures.

## 5 MARINE SCOUT II

The MARINE SCOUT II project was undertaken to convert the previous MARINE SCOUT I payload for use with copter-style UAVs and to improve the performance of the payload in terms of operating conditions and endurance (**Fig. 20** and **Fig. 21**). The following improvements were made to the previous payload:

- The LWIR camera was upgraded to a FLIR radiometrically calibrated EO/LWIR camera capable of reading pixel temperatures directly from the image.
- Additionally, the FLIR camera includes the following meta data with each image: GPS position, altitude, barometric pressure, inertial measurement unit, temperature, and humidity.
- The same SWIR sensor was used with a paddle filter, allowing SWIR and VNIR images to be taken.
- The payload was ruggedized to an approximate IP65 level (dust tight and resistant to low-pressure jets and moisture).
- The operational temperature range was extended from 15°F to 122°F, including a removal side panel to allow hot weather operation.
- An RGB camera was included to stream EO video for situational awareness.
- The communications were improved to simultaneously support WIFI and LTE signals to allow for high-bandwidth downlink communications.

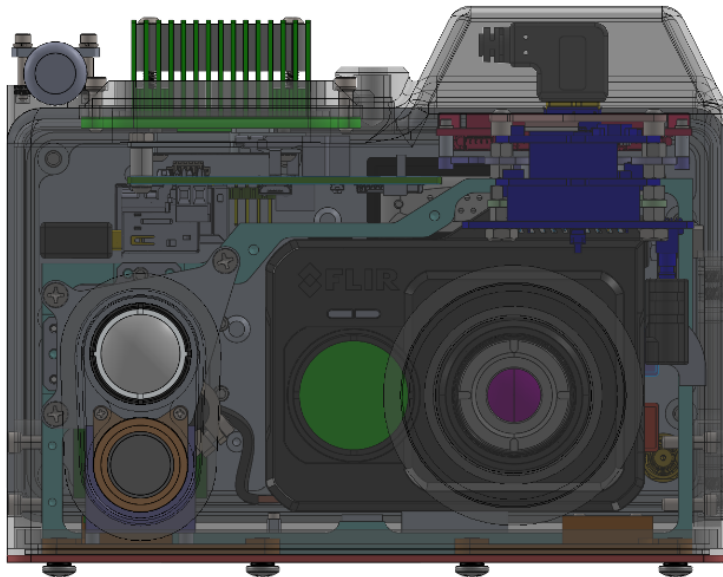


**Fig. 20** MARINE SCOUT II payload showing FLIR LWIR sensor, SWIR sensor, and EO video

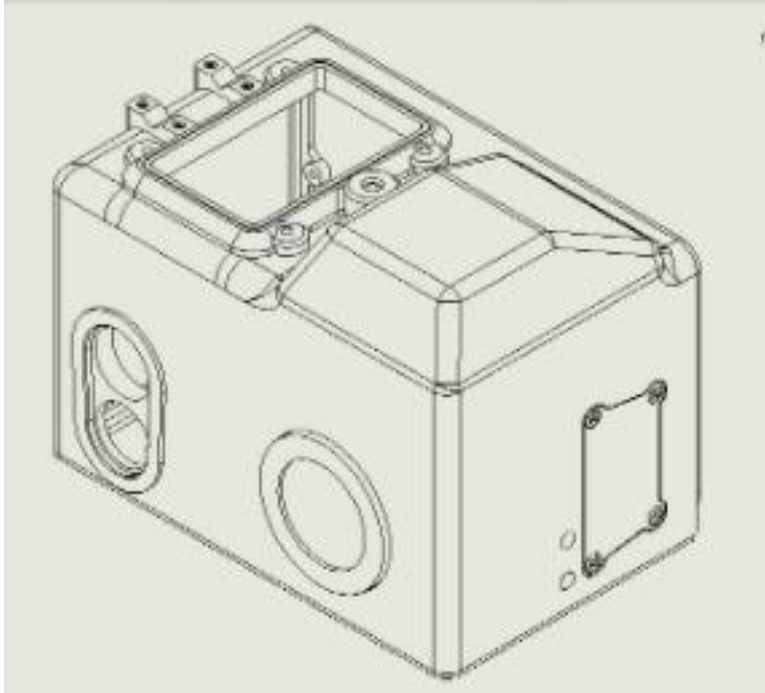


**Fig. 21 MARINE SCOUT II payload showing side weather panel and top heat sink**

## **5.1 System Design**

The MARINE SCOUT II system has the following components:

- Payload that supports LWIR, SWIR, and VNIR imagery and EO video.
- Payload supports WIFI and LTE downlink formats.
- Payload supports real-time image download and store-and-forward modes depending on the bandwidth of the downlink.
- Ground station supports WIFI and LTE formats, and interfaces in real-time to a Davis Instruments' Vantage Pro2 weather station and data logger.
- Ground station runs the oil depth and declutter algorithms in near-real-time. The algorithms are written in Python to allow for easy analysis and optimization.
- The UAV is the Skyfront Perimeter 8 UAV and is capable for flying for 3 hours and a 60-mile range while carrying the MARINE SCOUT II payload.



## 6 Flight Test

The MARINE SCOUT Advancement project concluded with a flight test at CRREL in Hanover, NH in May 2023. A total of 29 flights were planned over a 3-day period, including sunrise and sunset flights. Twenty-four flights were completed (five were canceled due to rain at the test facility).

### 6.1 CRREL

The CRREL facility in Hanover, NH (**Fig. 22**), is in Class G airspace, which means that FAA airspace authority is not needed for UAV flight operations below 400' ASL. Additionally, flights needed to be conducted in LOS mode during daylight hours (between sunrise and sunset), and not conducted off vehicles. Since the purpose of the flight test was to collect imagery and algorithm results from the oil targets in the CRREL test pool, these constraints were acceptable, and no FAA waivers were obtained.

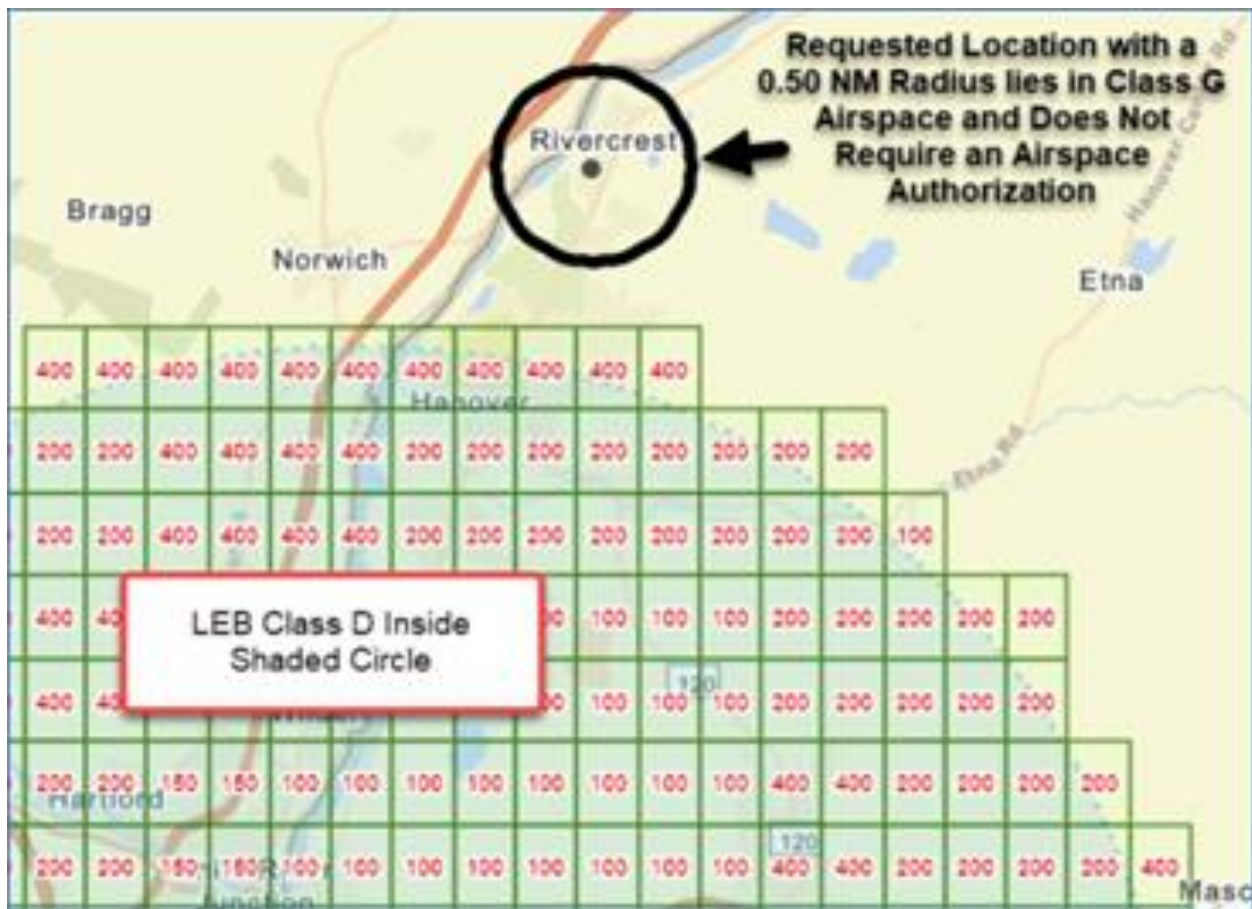


**Fig. 22** Airspace map of the CRREL location

The test facility at CRREL (**Fig. 23**) is a temperature-controlled test pool that optionally can be covered or open to the environment. For the purposes of this flight test, the pool was uncovered

and allowed to adapt to environmental conditions. The oil samples were placed the day before the first flight.



**Fig. 23 CRREL test pool location**

The oil targets were 1m in diameter and open to the pool shown in **Fig. 24**. There were 12 targets included in the tests: 10 for oil samples, 1 control, and 1 vegetative confuser.



Fig. 24 CRREL test pool at sunset showing oil targets and cover

## 6.2 Flight Test Plan

The flight test plan (including modifications and canceled flights) is shown in **Table 2**.

Flt #	Date/Time	Mode	Altitude	Dis/Dur	Flight Path	Payload	Objective
1	Mon 5/22, 10 a.m.	Manual	Various	15m	Site (VLOS)	P1	Shakeout flight (UAV, obstacles, comms, site)
2	Mon 5/22, 11 a.m.	Waypoint	100'-200'	20m	Ext target area	P1	Site sweep at 200', altitude sweep @ tank (100-200)
3	Mon 5/22, 11:30 a.m.	Waypoint	100'-200'	20m	Ext target area	P2	Site sweep at 200', altitude sweep @ tank (100-200)
4	Mon 5/22, 1:00 p.m.	Waypoint	200'	15m	Target area	P2	Circle tank @ 200', then hover over center for 5'
5	Mon 5/22, 2:00 p.m.	Waypoint	200'	15m	Target area	P1	Circle tank @ 200', then hover over center for 5'
6	Mon 5/22, 3:00 p.m.	Waypoint	200'	15m	Target area	P2	Circle tank @ 200', then hover over center for 5'
7	Mon 5/22, 4:00 p.m.	Waypoint	200'	15m	Target area	P1	Circle tank @ 200', then hover over center for 5'
8	Mon 5/22, 5:00 p.m.	Waypoint	200'	15m	Target area	P2	Circle tank @ 200', then hover over center for 5'

<b>Flt #</b>	<b>Date/Time</b>	<b>Mode</b>	<b>Altitude</b>	<b>Dis/Dur</b>	<b>Flight Path</b>	<b>Payload</b>	<b>Objective</b>
9	Tues 5/23, sunrise 5:17 a.m.	Waypoint	200'	20m	Ext target area	P2	Hover over tank @ 200', then site sweep
10	Tues 5/23, 7:00 a.m.	Waypoint	200'	15m	Target area	P1	Circle tank @ 200', then hover over center for 5'
11	Tues 5/23, 9:00 a.m.	Waypoint	200'	15m	Target area	P1	Circle tank @ 200', then hover over center for 5'
12	Tues 5/23, 11:00 a.m.	Waypoint	200'	20m	Ext target area	P1	Site lawn mower pattern – north/south
13	Tues 5/23, 1:00 p.m.	Waypoint	200'	20m	Ext target area	P1	Site lawn mower pattern – east/west
14	Tues 5/23, 2:00 p.m.	Waypoint	200'	15m	Target area	P1	New oil depths Optional: Repeat Flt #5 if weather conditions are different or if more hot imagery is needed
15	Tues 5/23, 3:00 p.m.	Waypoint	250'	15m	Target area	P1	Optional: Repeat Flt #6 if weather conditions are different or if more hot imagery is needed
16	Tues 5/23, 4:00 p.m.	Waypoint	150'	15m	Target area	P1	Optional: Repeat Flt #7 if weather conditions are different or if more hot imagery is needed
17	Tues 5/23, 6:30 p.m.	Waypoint	300'	20m	Ext target area	P1	Hover over tank @ 200', then site sweep
18	Tues 5/23, sunset (start: 7.54p.m.)	Waypoint	200'	10m	Target area	P1	Hover over tank @ 200' for 5'
19	Wed 5/24, sunrise 7:00 a.m.	Waypoint	200'	20m	Ext target area	P1	Optional: Repeat Flt #9 if more data is needed
20	Wed 5/24, 9:00 a.m.	Waypoint	100'-400'	20m	Target area	P1	Full altitude sweep – 100'-400' in 25' increments
21	Wed 5/24, 10 a.m.	Waypoint	300'	15m	Ext target area	P1	Circle tank @ 200', then hover over center for 5'
22	Wed 5/24, 11:00 a.m.	Waypoint	300'	15m	Ext target area	P2	Lawnmower
23	Wed 5/24, 12:00 a.m.	Waypoint	300'			P1	Lawnmower
24	Wed 5/24, 1:00 a.m.	Waypoint	300'			P1	Circle and hover

Generally, the flights were conducted in waypoint flight mode at 200' and followed certain paths. The strategy was to collect target data at different times in different conditions, and to collect the target data from a variety of positions and altitudes over the course of the field trial (**Fig. 25**).



**Fig. 25 CRREL flight test – flight paths used for trials**

Operationally, the “lawn mower” flight path is the most likely to be used in real-world collection scenarios, so that was done at CRREL even though the entire flight was conducted with sight of the test pool, launch point, and ground station.

The flight test team was comprised of a pilot, a payload ground station operator, an algorithm operator, and three flight observers. The UAV flew in LOS conditions on all the flights. For field deployments, the system could be fielded with a pilot and payload ground station operator.

### 6.3 CRREL Target Configuration

There were 12 targets placed in the test pool. One was a control with nothing in it, and one was a vegetative confuser that contained local leaf debris. The remaining 10 targets were split between ANS crude and HOOPS crude (Fig. 26).

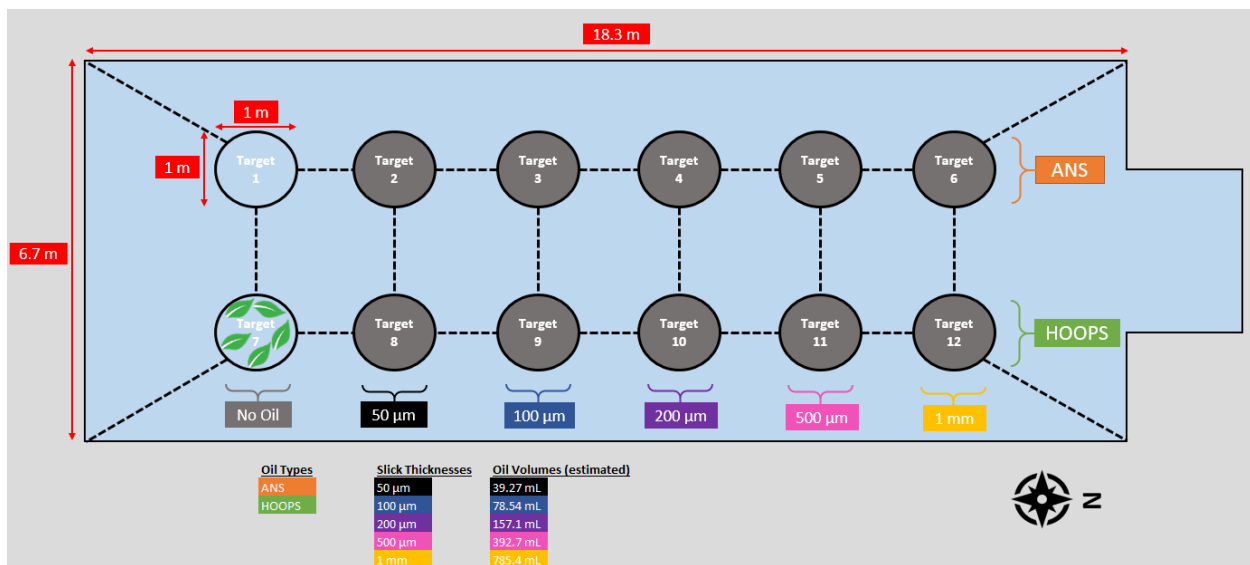


**Fig. 26 CRREL target pool configuration**

The oil thicknesses used are shown in Table 3. Midway through the field trial, the oil thicknesses were increased, and two of the targets converted to mystery thicknesses to test the effectiveness of the algorithms.

Target #	Oil Type	Oil Thickness
1	No Oil	Open Water
2	ANS	50 $\mu\text{m}$
3	ANS	100 $\mu\text{m}$
4	ANS	200 $\mu\text{m}$
5	ANS	500 $\mu\text{m}$
6	ANS	1 mm
7	No Oil	Seaweed (confuser)
8	HOOPS	50 $\mu\text{m}$
9	HOOPS	100 $\mu\text{m}$
10	HOOPS	200 $\mu\text{m}$
11	HOOPS	500 $\mu\text{m}$
12	HOOPS	1 mm

The oil in the target containers clumped into swirls at lower oil concentrations where the oil thickness obviously varied over the surface of the target. This could be visualized in lower altitude flights and might serve to explain some of the thickness variances calculated by the algorithms (Fig. 27).



Fig. 27 CRREL test pool with oil targets

The water conditions during the test were monitored by CRREL personnel and are shown in Fig. 28.

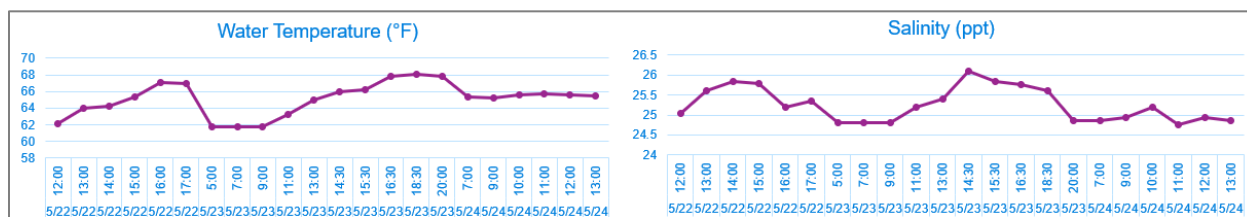


Fig. 28 CRREL test conditions

## 6.4 Results

### 6.4.1 Unknown Oil Depth Identification

After flight #13, the additional oil was added to the oil targets. Targets #2 and #8 had an unknown amount of oil added in order to check on the accuracy of the algorithms. Flight #14

was conducted at 200' altitude at 2:29 p.m. with low cloud cover. The resulting oil depth map is shown in **Fig. 29**.

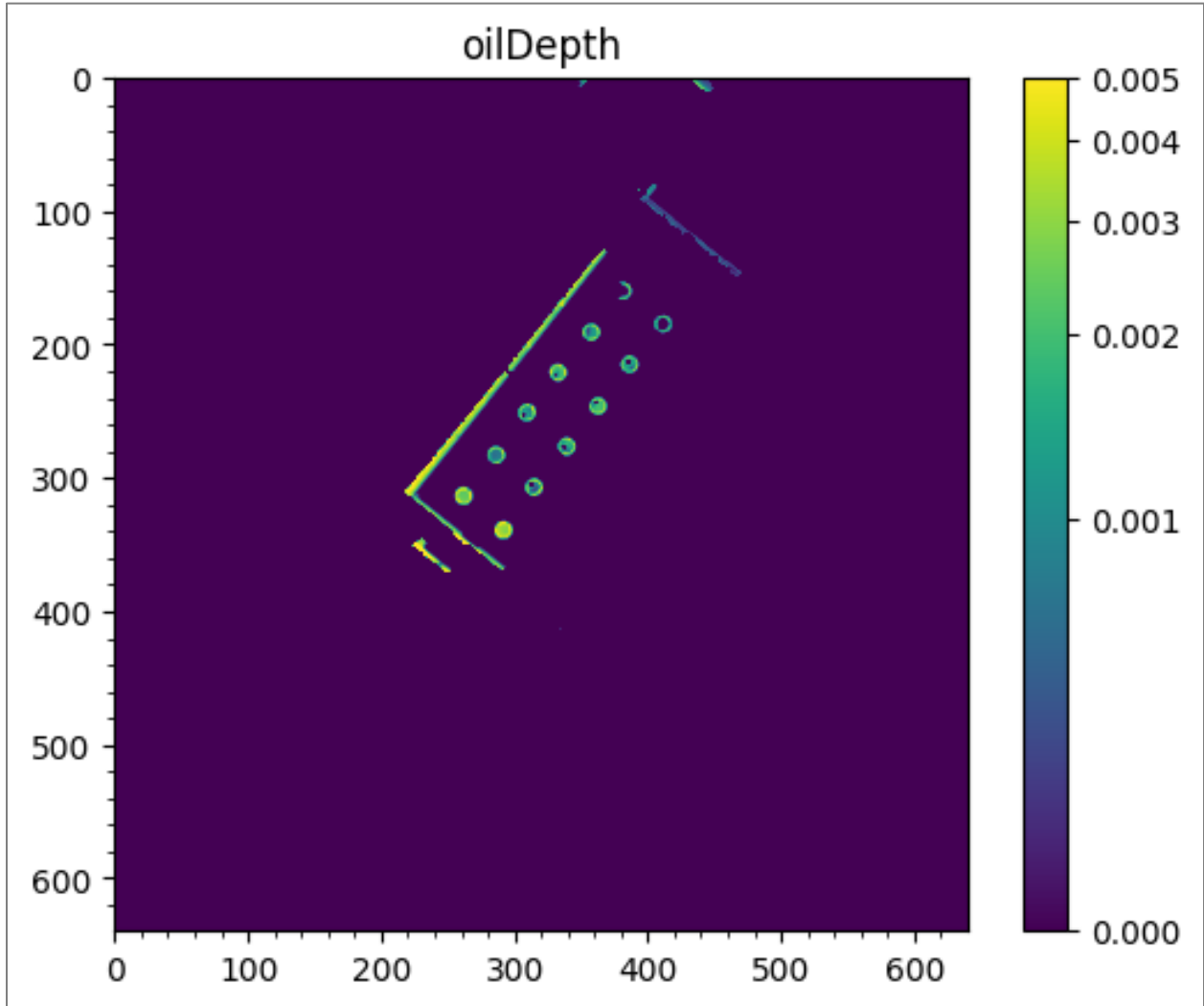


**Fig. 29** CRREL mystery oil depth results

The calculated results are shown in **Fig. 30**. The algorithms hit one of the two unknown targets exactly and only missed on the second one by 0.1mm.

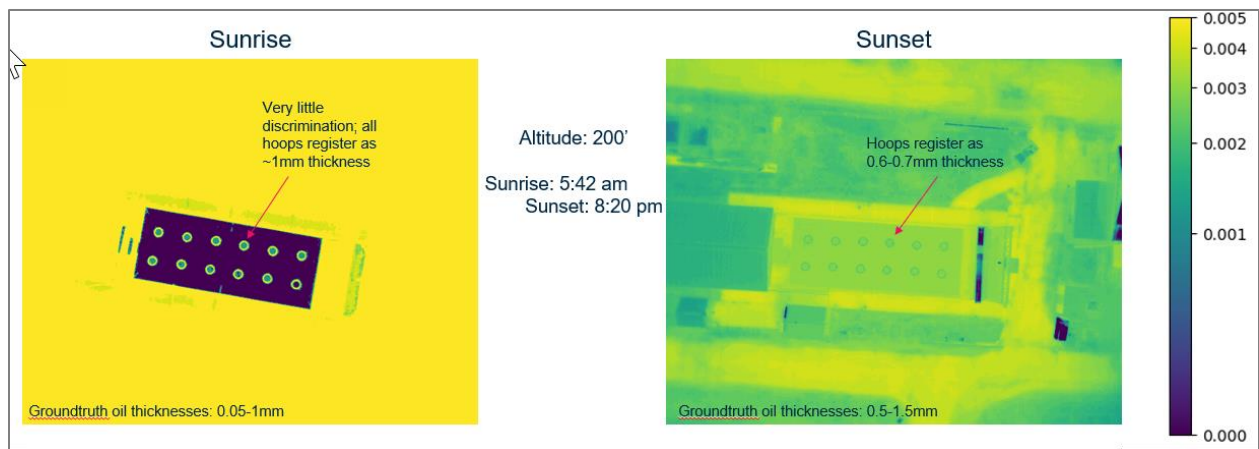
Unrevealed "mystery" thickness ↓						
<b>GROUNDTRUTH</b>						
1mm	0.5mm	0.7mm	1.5mm	1.2mm	Confuser	HOOPS
1mm	0.5mm	0.7mm	1.5mm	1.2mm	Control	ANS
<b>CALCULATED</b>						
2mm	0.6mm	0.9mm	1.8mm	1.2mm	*none*	HOOPS
3mm	0.4mm	1.2mm	2mm	1.3mm	*none*	ANS

Fig. 30 Ground truth vice calculated results

### 6.4.2 Twilight Collection

For the sunrise and sunset collections, the SWIR images are undersaturated and not suitable for use in finding the region(s) of interest in the co-registered images. Therefore, the LWIR image is subjected to clustering, and then the nighttime oil depth algorithm is run. In general, the nighttime algorithm flattens the image so the variance in target depths is much less than ground truth (Fig. 31).





**Fig. 31 CRREL sunrise and sunset algorithm results**

Sunset and sunrise are close to the temperature crossover zone, so it's possible that the oil temperature is close to the water temperature, which could lead to ambiguous results.

### 6.4.3 Altitude Comparison

Some of the flights performed altitude sweeps where the UAV was stationed at the same spot but at various altitudes. The purpose of this was to determine the most effective altitude for data collections. **Fig. 32** shows data collected at 100', 200', 300', and 400'.

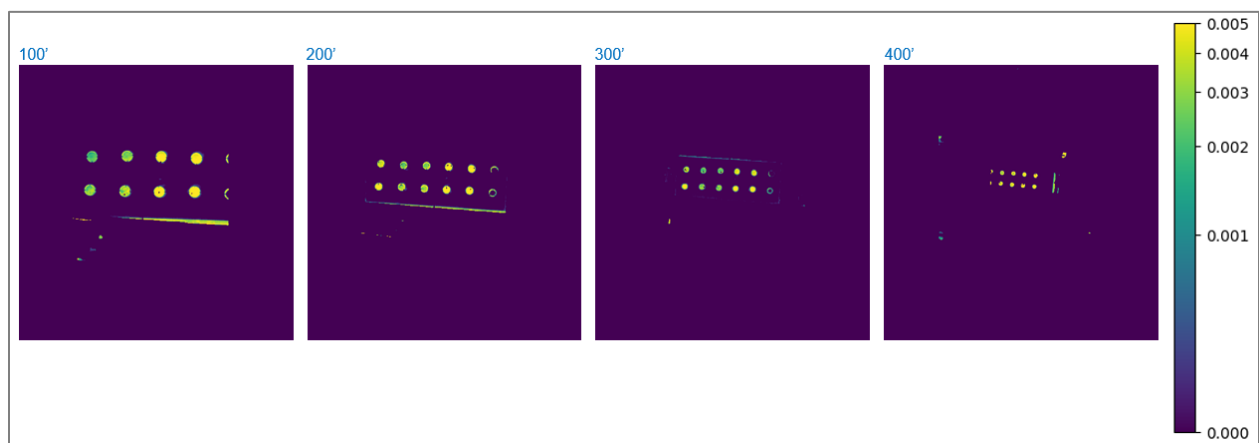


**Fig. 32 CRREL altitude sweep at 9:00 a.m. with moderate cloud cover**

At the higher altitude, the oil temperature can still be determined, but there are not many pixels on target for a 1m diameter oil target. Operationally this could present issues, although typically oil spills are much greater than 1m in diameter. The P8 UAV can fly to over 10,000' in altitude, so it should be possible to detect large oil sheens as even a small number of pixels on target can be detected. For this collection, the oil depth readings are very similar for the 100', 200', and 300' data.

#### 6.4.4 Water Temperature Determination

For both the daytime and nighttime oil depth algorithms to work, they need a measurement of the water temperature for water not covered in an oil sheen. We developed two methods for this measurement. For image sets with good SWIR images, we used K-Means clustering to identify the water regions in the imagery and mask out everything else. Then we used the LWIR algorithm to read the temperature of every pixel in the region and took an average to get the approximate water temperature. If the SWIR image is not of sufficient quality, the LWIR image was clustered using K-Means clustering, and the average temperature of the coldest region was taken as the approximate water temperature. Both methods have some drawbacks, but we wanted an approach that did not require operator intervention to work. **Fig. 33** shows some sample results of this approach.

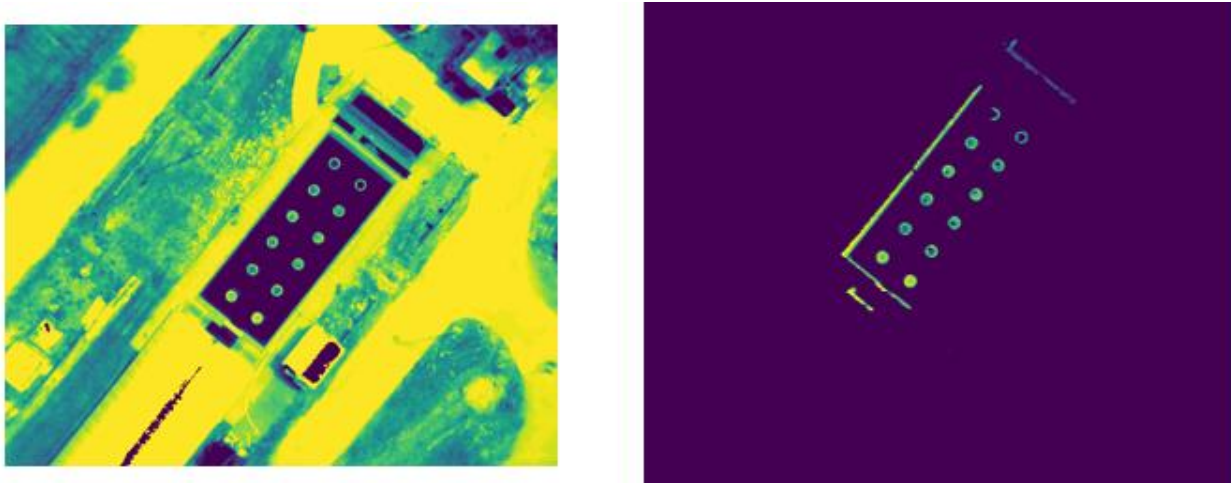


**Fig. 33** CRREL water temperature determination (LWIR approach on the left, SWIR approach on the right)

Using the water temperature as determined above, the depth algorithm was run on the oil targets with the results shown in **Fig. 34**.

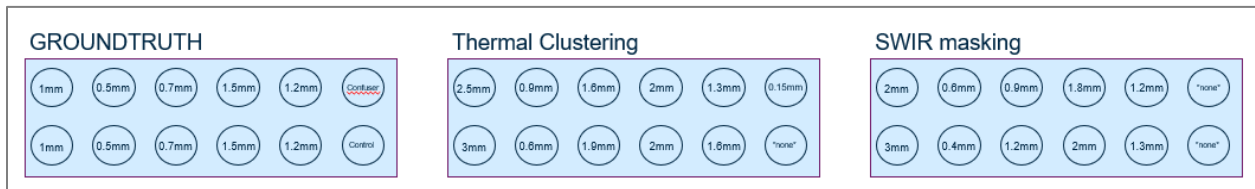


**Fig. 34** CRREL oil depth using different water temperature determination approach

Based on these results, the preferred approach is to use the SWIR clustering if possible.

#### 6.4.5 Confuser Identification and Masking

For all of the flights, target-#7 contained a vegetative confuser. **Fig. 35** provides a sample of the confuser getting masked out of the final oil depth map. The raw LWIR image collected does not show much differentiation between target #7 and the other oil targets.

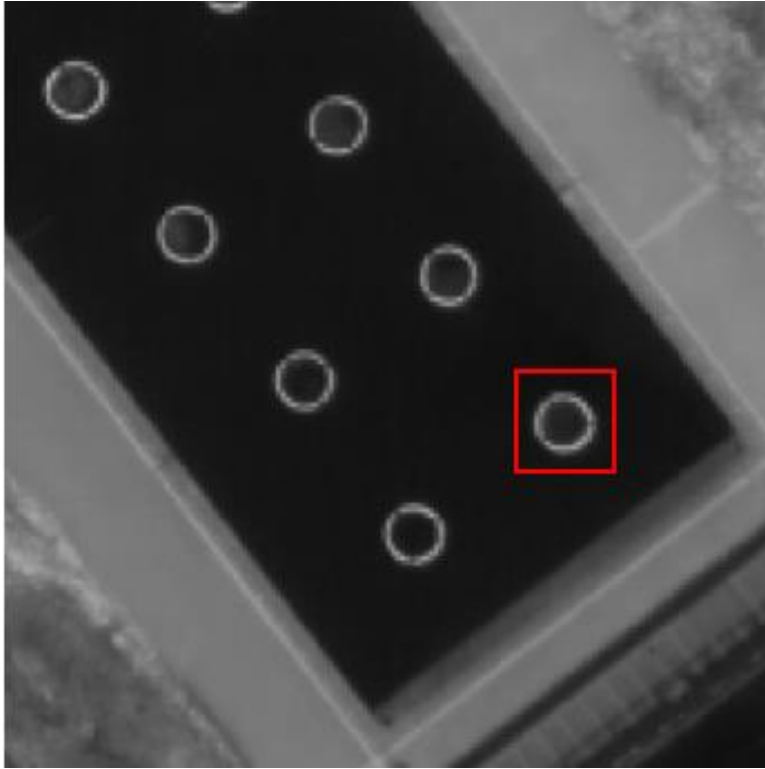


**Fig. 35 CRREL LWIR image showing confuser target**

When the SWIR clustering is used, the confuser is clustered with other terrain features and masked out for the oil depth algorithm (**Fig. 36**).

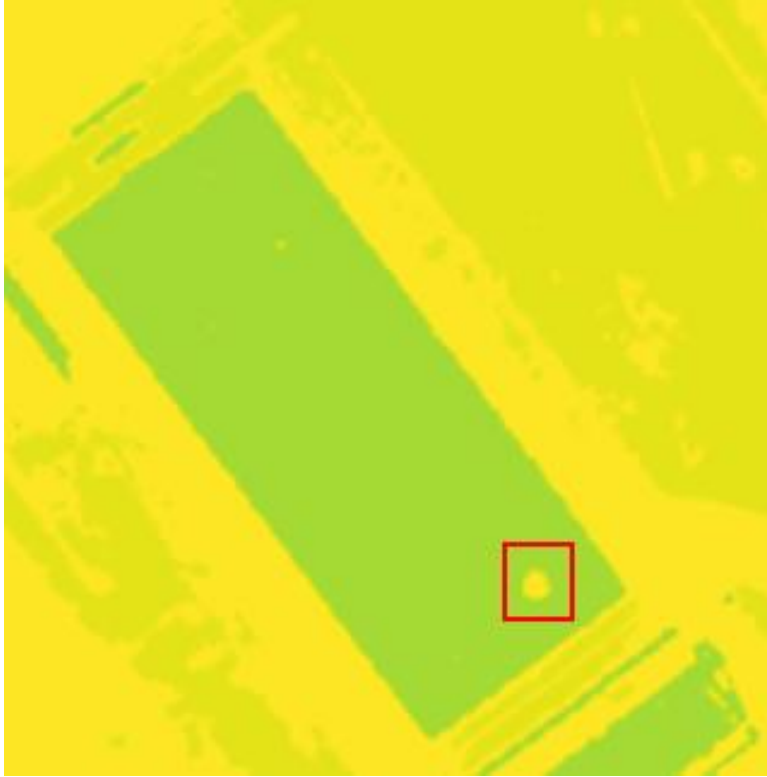


**Fig. 36 CRREL clustered SWIR image showing confuser clustered with terrain**

With the mask in place, the oil depth algorithm ignores the contents of the confuser target (**Fig. 37**).

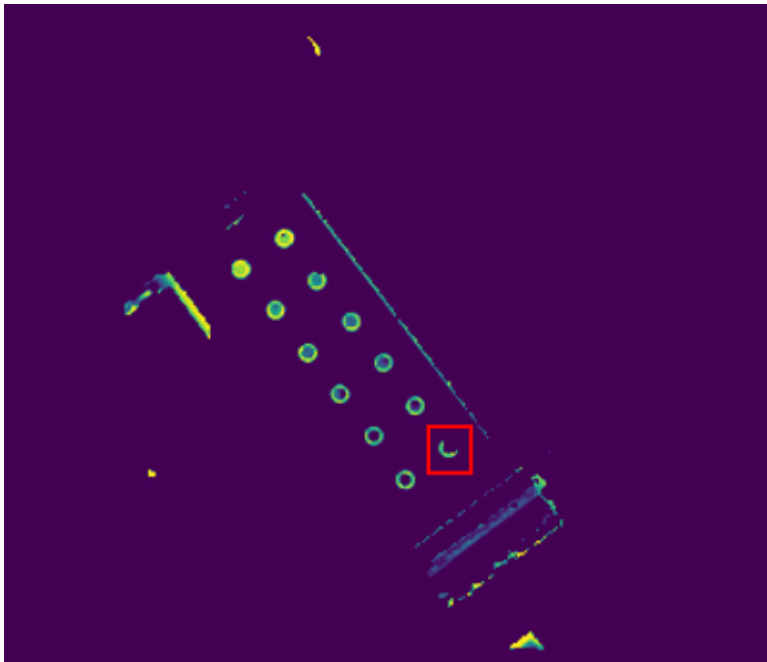


**Fig. 37 CRREL final oil depth map showing that confuser is masked out**

### 6.4.6 Water vs Terrain Identification

There is a pond near the test pool at the CRREL facility. We obtained some imagery of it during the lawnmower flights (**Fig. 38**). The SWIR algorithm was able to detect the pond as a region of interest, even though the test pool was not present in the imagery.



**Fig. 38** CRREL UAV launch site with pond nearby

**Fig. 39** contains the raw LWIR images containing the pond and the co-registered clustered SWIR image on top of the LWIR image showing the pond as a region of interest.

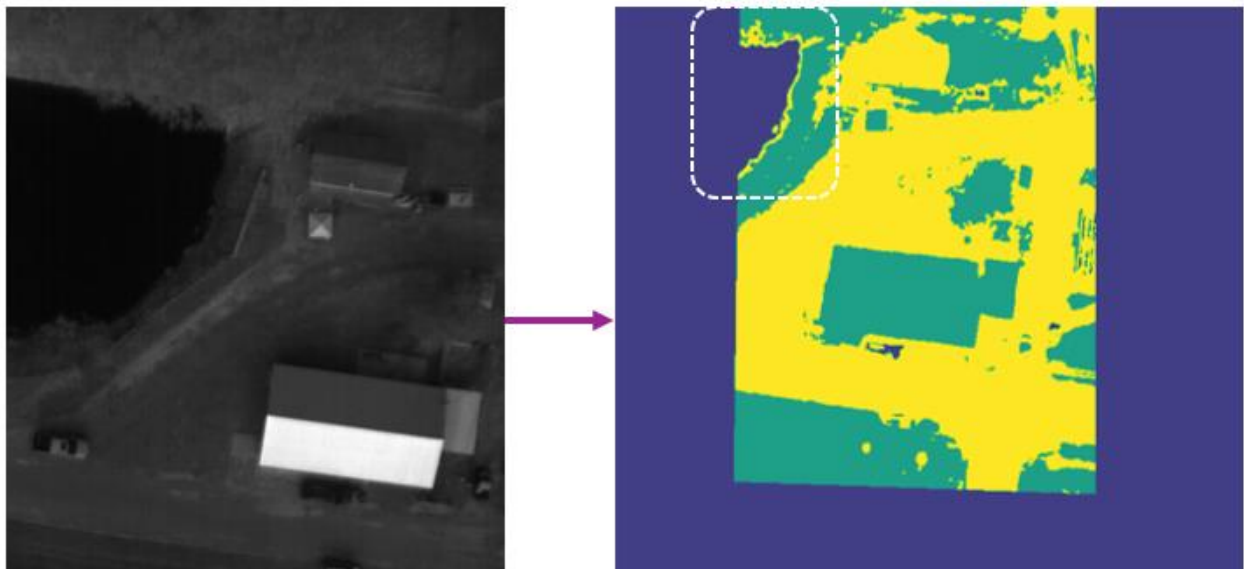


**Fig. 39** CRREL – Pond is detected as a region of interest by the SWIR clustering algorithm

### 6.4.7 Sample Flight Test Results

Fig. 40, Fig. 41, Fig. 42, Fig. 43, Fig. 44, and Fig. 45 show full sets of imagery captured on several flights throughout the 3-day test event.

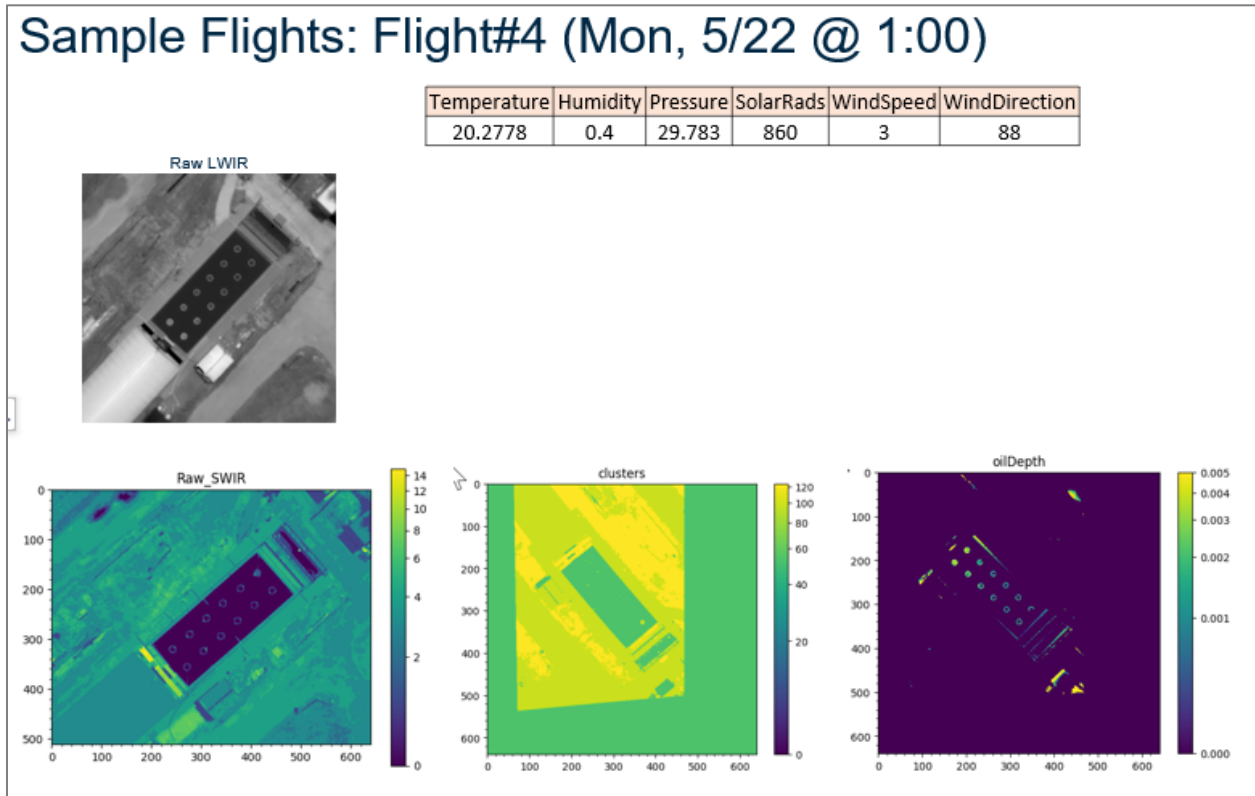


Fig. 40 Flight #4 results

# Sample Flights: Flight#7 (Mon, 5/22 @ 4:00PM)

Temperature	Humidity	Pressure	SolarRads	WindSpeed	WindDirection
22.2222	0.32	29.75	568	3	90

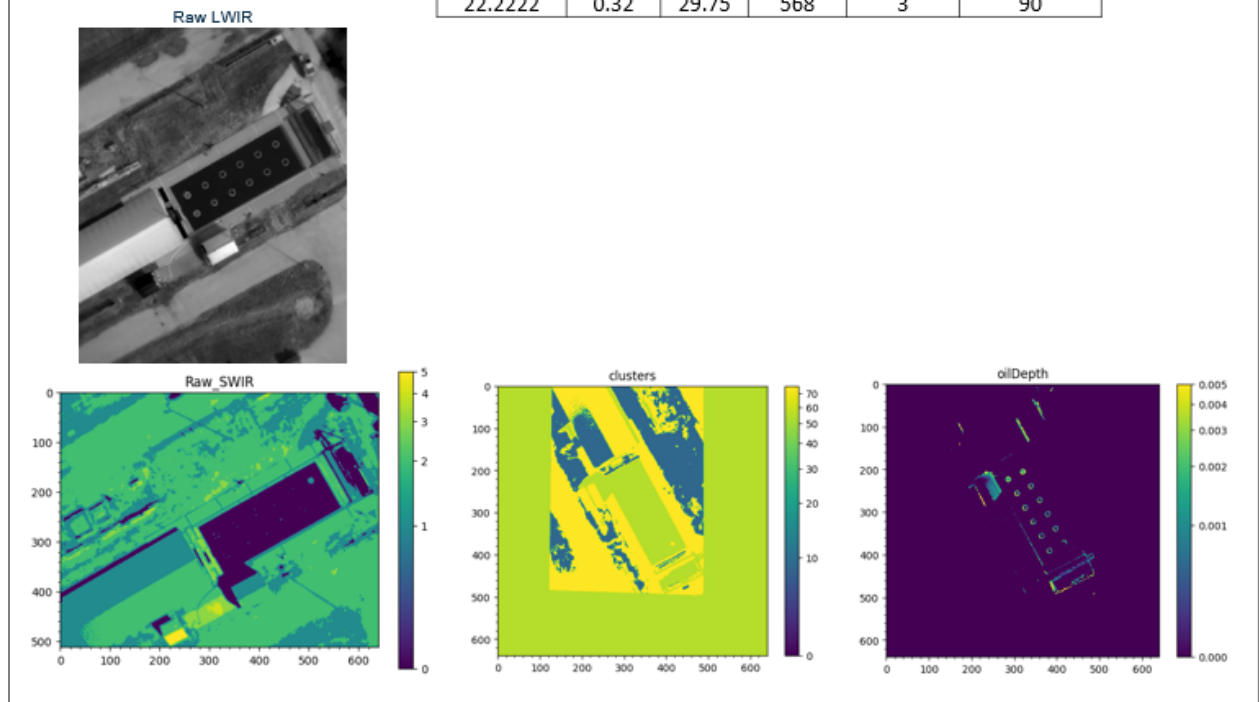


Fig. 41 Flight #7 results

# Sample flights – Flight#9 (Tues, 5/23 @ Sunrise (5:23AM))

Temperature	Humidity	Pressure	SolarRads	WindSpeed	WindDirection
5.16667	0.89	29.921	25	0	45

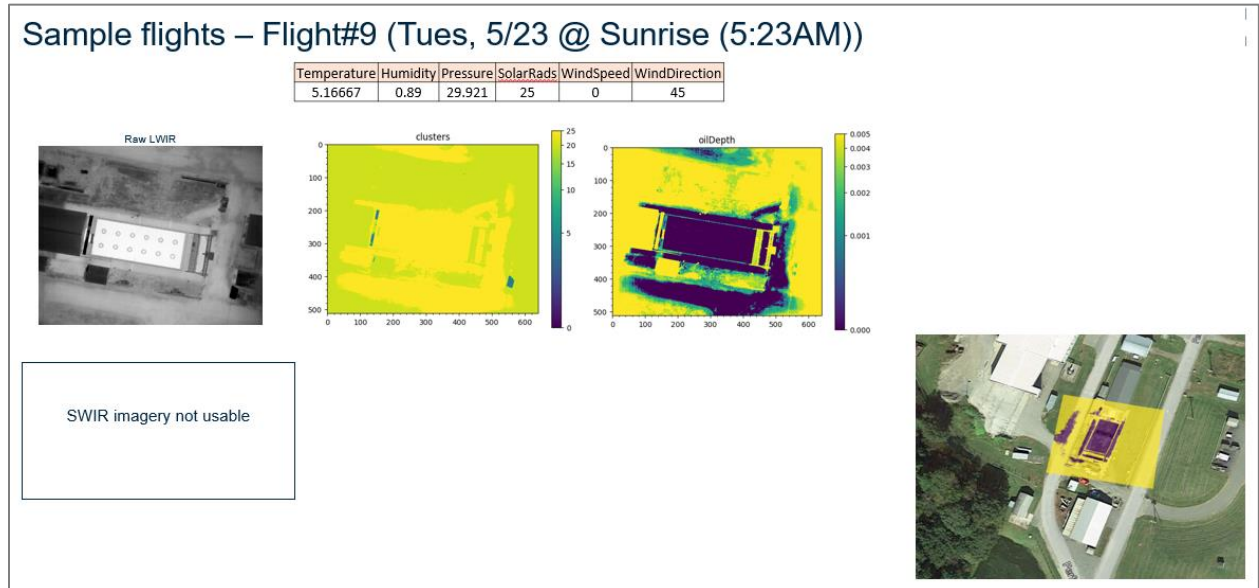


Fig. 42 Flight #9 results

### Sample Flights: Flight#12 (Tues 5/23 @ 9:00AM)

Temperature	Humidity	Pressure	SolarRads	WindSpeed	WindDirection
18.0556	0.53	29.904	814	2	188

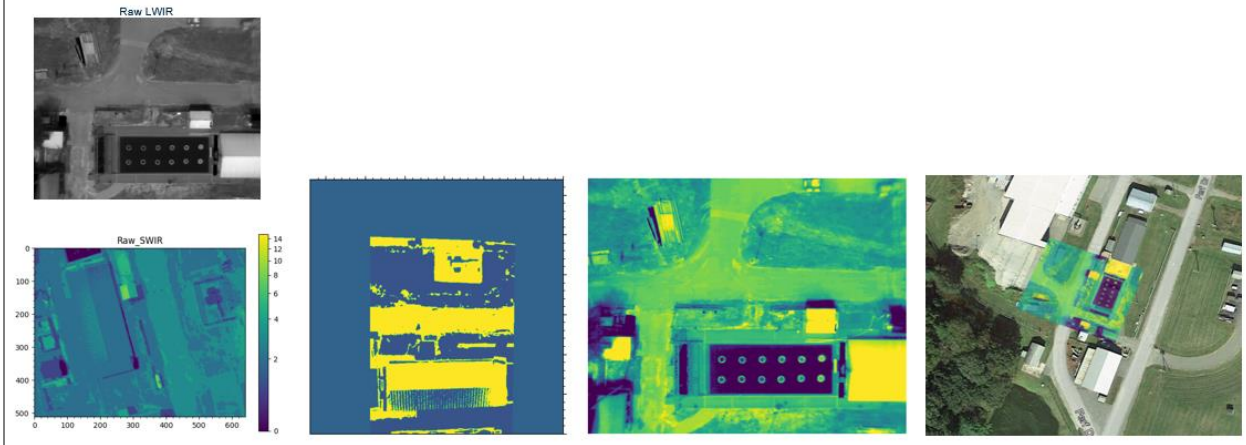


Fig. 43 Flight #12 results

### Sample Flights: Flight#18 (Tues, 5/23 @ Sunset (7:54PM))

Temperature	Humidity	Pressure	SolarRads	WindSpeed	WindDirection
24.3333	0.42	29.772	638	4	217

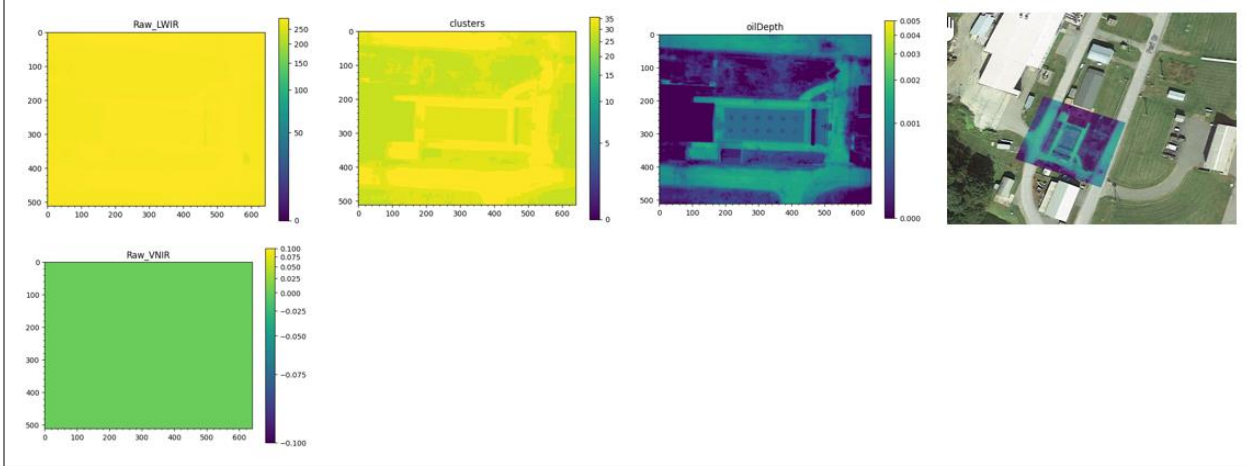


Fig. 44 Flight #18 results



# Sample Flights: Flight#20 (Wed, 5/24 @ 9:00AM)

Temperature	Humidity	Pressure	SolarRads	WindSpeed	WindDirection
15.3889	0.61	29.616	302	3	275

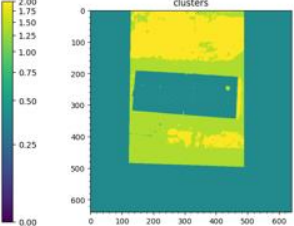
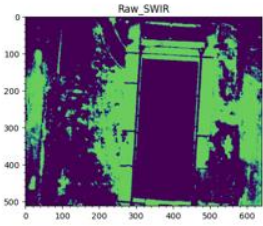


Fig. 45 Flight #20 results

## 7 Conclusions

Initially, the MARINE SCOUT Advancement project set out to reconfigure and ruggedize the payload, and then later sought to re-create Toomas Allik's algorithms and optimize their performance. In the end, the payload met the targets for its size, weight, and power (**Table 4**).

<b>Table 4 Specifications</b>		
<b>SWAP</b>	<b>MARINE SCOUT Requirement</b>	<b>Results</b>
Size	Compatible with P8 UAV and GremsyT7 gimbal	✓
Weight	Maximum weight threshold: 7.5 lbs	Payload: 3.64 lbs, gimbal: 3.8 lbs, so the total weight is 7.44 lbs (✓)
Power	100W at 48V	Avg: 17.4W, peak: 26.1W (✓)

The payload has a wide operating temperature range and is ruggedized (IP65) to be sealed vs dust and resistant to moisture and spray.

From an algorithm performance standpoint, the MARINE SCOUT II algorithms performed consistently well throughout the 3-day CRREL field trial. The K-Means clustering used with the SWIR and VNIR images was reliably able to detect the water and water/oil regions of interest, and the resulting constraint mask was able to reduce the clutter in the LWIR images such that oil areas and thicknesses were easy to identify.

The oil depth algorithm was able to consistently calculate approximate oil thicknesses and, in many cases, get it exactly right. It worked better in good sunlight conditions, and generally skewed thicker in its calculations than for ground truth.

The SWIR/VNIR imagery degraded in quality quickly in low lighting, heavy overcast, or rainy conditions and was generally not usable during those times or for the nighttime oil calculations. The LWIR daytime algorithm continued to perform acceptably in those conditions, though it had to be run against the entire image.

The oil depth algorithm used did not take into account the type of oil expected, so variances due to the type of oil were not accounted for, and no data was collected during civil twilight or true night conditions.

## 8 Future Work

There are many areas of interest for additional work. The first is to convert the payload for use on a Blue Drone Government-approved UAV system. Both the current gimbal and the MARINE SCOUT II payload mount in standard ways, so physically converting for use with another UAV should be straightforward. Converting the power inputs and communications interfaces will be more challenging. Also, the FLIR LWIR sensor in the payload is sensitive to vibration (reported by FLIR on a unit we sent back for repair) and should be remounted to include strain relief. Also, operationally the FLIR sensor does not respond consistently to external triggers, so some work will have to be done to improve its reliability in the payload to align the FLIR imagery with the SWIR and VNIR imagery.

From an algorithm perspective, the current algorithms work well enough to be field-tested in real-world scenarios (i.e., the oil seeps off Santa Barbara, Alaska, or the Gulf of Mexico) and for long-duration, NLOS flights. Additionally, the current algorithms work well enough to score imagery (can create zones for water or water/oil mixes vs. terrain or waterborne confusers). Scored imagery can be used to train machine-learning algorithms, which might offer superior performance at identifying oil sheens and calculating their thicknesses.

Another avenue for future work would be to have the algorithms tuned to run automatically on receipt of imagery from the payload. That way, direct feedback from the mission flight plan to the payload operator (including situational awareness video) would be possible, allowing the mission plan to adapt live to conditions discovered during the flight.

## 9 References

Allik, Toomas H. 2015 Dec 15. Enhanced Oil Spill Detections Sensors in Low-Light Environments. Bureau of Safety and Environmental Enforcements.

Myhr, Scot; Ax, George; Gill, John; LeClair, Lance; Sippel, Evan; Walters, Mark; Allik, Toomas H; Dixon, Roberta. 2018 Apr. Mapping and Reconnaissance Imager, Night-Enhanced, for Sensing of Contaminants, Oil, and Unseen Threats (MARINE SCOUT). Bureau of Safety and Environmental Enforcements.

Allik, Toomas H; Dixon, Roberta; Walters, Mark. 2018 Feb 15. Remote Measurement of Thick Oil Spill Depth using Thermal Imagery. Bureau of Safety and Environmental Enforcements.

## 10 Abbreviations and Acronyms

ANS	Alaska North Slope
ASL	Above Sea Level
BSEE	Bureau of Safety and Environmental Enforcement
CO	Contracting Officer
COR	Contracting Officer's Representative
CRREL	Cold Regions Research and Engineering Laboratory
DDL	Digital Data Link
DOI	Department of the Interior
DVE	Degraded Visual Environment
EO	Electro-Optical
FLIR	Forward-Looking Infrared
FMV	Full-Motion Video
FOV	Field of View
GPS	Global Positioning System
HOOPS	Hoover Offshore Oil Pipeline System
KML	Keyhole Markup Language
LOS	Line of Sight
LTE	4G Cellular System
LWIR	Long-Wave Infrared
MWIR	Mid-Wave Infrared
NIR	Near-Infrared
NLOS	Non-Line-of-Sight
OSPD	Oil Spill Preparedness Division
OSRR	Oil Spill Response Research
SUAS	Soldier Unmanned Aircraft System
SWIR	Short-Wave Infrared
UAS	Unmanned Aerial System
UAV	Unmanned Aerial Vehicle
VLOS	Visual Line-of-Sight
VNIR	Visible and Near-Infrared
WIFI	802.11 Wireless Ethernet



## **Department of the Interior (DOI)**

The Department of the Interior protects and manages the Nation's natural resources and cultural heritage; provides scientific and other information about those resources; and honors the Nation's trust responsibilities or special commitments to American Indians, Alaska Natives, and affiliated island communities.



## **Bureau of Safety and Environmental Enforcement (BSEE)**

The mission of the Bureau of Safety and Environmental Enforcement works to promote safety, protect the environment, and conserve resources offshore through vigorous regulatory oversight and enforcement.

### **BSEE Oil Spill Preparedness Program**

BSEE administers a robust Oil Spill Preparedness Program through its Oil Spill Preparedness Division (OSPD) to ensure owners and operators of offshore facilities are ready to mitigate and respond to substantial threats of actual oil spills that may result from their activities. The Program draws its mandate and purpose from the Federal Water Pollution Control Act of October 18, 1972, as amended, and the Oil Pollution Act of 1990 (October 18, 1991). It is framed by the regulations in 30 CFR Part 254 – *Oil Spill Response Requirements for Facilities Located Seaward of the Coastline*, and 40 CFR Part 300 – *National Oil and Hazardous Substances Pollution Contingency Plan*. Acknowledging these authorities and their associated responsibilities, BSEE established the program with three primary and interdependent roles:

- Preparedness Verification,
- Oil Spill Response Research, and
- Management of Ohmsett - the National Oil Spill Response Research and Renewable Energy Test Facility.

The research conducted for this Program aims to improve oil spill response and preparedness by advancing the state of the science and the technologies needed for these emergencies. The research supports the Bureau's needs while ensuring the highest level of scientific integrity by adhering to BSEE's peer review protocols. The proposal, selection, research, review, collaboration, production, and dissemination of OSPD's technical reports and studies follows the appropriate requirements and guidance such as the Federal Acquisition Regulation and the Department of Interior's policies on scientific and scholarly conduct.